

Opportunistic Routing Aided Cooperative Communication Network with Energy Harvesting

Wannian An, Chen Dong*, Xiaodong Xu, Chao Xu, Shujun Han, and Lei Teng

Abstract—In this paper, a cooperative communication network based on energy-harvesting (EH) decode-and-forward (DF) relays that harvest energy from the ambience using buffers with harvest-store-use (HSU) architecture is considered. An opportunistic routing (OR) protocol, which selects the transmission path of packet based on the node transmission priority, is proposed to improve data delivery in this network. Additionally, an algorithm based on state transition matrix (STM) is proposed to obtain the probability distribution of the candidate broadcast node set. Based on the probability distribution, the existence conditions and the theoretical expressions for the limiting distribution of energy in energy buffers using discrete-time continuous-state space Markov chain (DCSMC) model are derived. Furthermore, the closed-form expressions for network outage probability and throughput are obtained with the help of the limiting distributions of energy stored in buffers. Numerous experiments have been performed to validate the derived theoretical expressions.

Index Terms—Energy-harvesting, opportunistic routing, state transition matrix, integral equation.

I. INTRODUCTION

IN recent years, as a promising technology, energy-harvesting (EH) has drawn researchers' substantial attention due to its capability of harvesting energy from the surrounding ambient energy sources such as light energy, thermal energy and radio frequency (RF) energy, etc. [1]. Specifically, EH is widely employed in cooperative wireless communication to prolong the lifetime of traditional energy-constrained cooperative wireless communication networks [2].

The relay selection method considering both the energy state of relay buffer and channel state information (CSI) for EH wireless body area network is shown in [3]. In [4] and [5], the power splitting protocol is employed at the EH relay of the EH-based cooperative communication network to obtain a tradeoff between the transmission energy and decoding energy. In these studies mentioned above, the energy is harvested with the harvest-use (HU) structure, which means that the harvested energy will be used immediately.

Another efficient method of harvesting energy from the environment is to use the harvest-store-use (HSU) architecture, which allows the harvested energy to be stored in an energy buffer or super-capacitor for later use. A wireless powered

communication system with an EH node using HSU architecture, which harvests energy from the RF signals in the downlink and uses the stored energy to transmit data in the uplink, is considered in [6], [7] and [8], where the limiting distribution of stored energy in energy buffer at the EH node is derived using discrete-time continuous-state space Markov chain (DCSMC) model. The online and offline optimization algorithms for joint relay selection and power control have been discussed in [9], which aim to maximize the end-to-end system throughput under the constraints of data and energy storage. In [10], an EH-based two-way relaying network is studied, where the relay uses the energy harvested from ambient RF signals to drastically reduce the battery energy consumption. In [11], two time switching policies of the EH relay equipped with energy and data buffers are proposed to maximize the throughput of the cooperative wireless network. To improve the performance of the energy-constrained cooperative communication network, [12] proposes a relay selection scheme based on the status of both energy buffer and data buffer. A cooperative cognitive radio network with two Internet of Things (IoT) devices serving as the relays has been investigated in [13], where the IoT devices employ a time-splitting-based approach for harvesting energy from the RF signals received from a pair of primary users and processing information. Furthermore, the exact expressions of outage probability for the IoT cooperative communication system under Nakagami-m fading is derived.

In these works mentioned above, when the path loss in practical communication link is high, it is not efficient for the relays to harvest energy from RF signals received from the source nodes [14]. Another strategy with greater practical interest is to build the self-sustaining node (SSN) which harvests energy from the ambience. More explicitly, the two-hop relay networks with an HSU-architecture-based EH relay are considered in [15], [16] and [17], where the theoretical expressions for the limiting distribution of energy stored in buffer employing best-effort and on-off policies are derived to analyze the system outage probability and throughput. Different from [16], a feedback strategy is introduced into the system considered in [17], which further improves the spectral efficiency of the system. Furthermore, [18] and [19] introduce the two-hop relay networks with a self-sustaining source and a self-sustaining relay, where both the source and the relay harvest energy from the ambience. In [20] and [21], the performance of a two-hop relay network with a self-sustaining source harvesting energy from the ambience and a data buffer-aided relay is analyzed, where three simple link selection schemes based on buffer status or channel knowledge

This work was supported in part by ~. (Corresponding author: Chen Dong.) Wannian An, Chen Dong, Xiaodong Xu, Shujun Han and Lei Teng are with the State Key Laboratory of Networking and Switching Technology, Beijing University of Posts and Telecommunications, Beijing, 100876, China. (e-mail: anwannian2021@bupt.edu.cn; dongchen@bupt.edu.cn; xuxiaodong@bupt.edu.cn; hanshujun@bupt.edu.cn; tenglei@bupt.edu.cn;).

Chao Xu is with the School of Electronics and Computer Science, University of Southampton, SO17 1BJ Southampton, U.K. (e-mail: cx1g08@ecs.soton.ac.uk).

are adopted to maximize the throughput of the relay network.

It can be found that the above studies are mainly based on a wireless two-hop relay network with relays with the same priority (i.e. they cannot communicate with each other). However, the practical wireless cooperative network often utilizes the wireless multi-hop network with distributed topology, such as the sensor network [22]. For the sake of further improving performance, the wireless multi-hop network based on opportunistic routing (OR) protocol has been widely studied. Specifically, an efficient OR protocol based on both cross-layer information exchange and energy consumption in an ad hoc network has been studied in [23] and [24]. Additionally, the OR protocol considering both global optimization and local optimization is proposed for the dependent duty-cycled wireless sensor network to minimize the end-to-end latency [25]. In order to realize the tradeoff between routing efficiency and computational complexity, multi-objective optimization and Pareto optimality are introduced into the power control-based OR for wireless ad hoc networks [26]. In [27], the OR utilizing the network-based candidate forwarding set optimization scheme is introduced to reduce the transmission delay and avoid duplicate transmission in wireless multi-hop networks. In order to reduce the energy consumption and improve the data delivery ratio in underwater wireless sensor networks, Coutinho and Boukerche [28] design two candidate set selection heuristics to jointly select the most suitable acoustic modem and next-hop forwarder candidate nodes for the current hop. Furthermore, in [29], a reliable reinforcement learning-based OR is proposed in the underwater acoustic sensor network.

According to the above researches, it can be easily found that although EH and OR have been widely studied in cooperative wireless networks, less attention has been devoted to the joint application of EH and OR in cooperative wireless networks. This article aims to study OR-aided cooperative communication networks with EH. Table I shows the comparison between our work and the above references. More specifically, decode-and-forward (DF) relays are powered by harvested energy from the ambience using the infinite-size buffers with HSU architecture. Additionally, the DCSMC model is used to model energy buffers. The main contributions of this work are as follows:

- 1) In this paper, a cooperative communication network based on EH DF relays is considered. In order to improve the data delivery in this network, an OR protocol for selecting the packet transmission path based on the node transmission priority is proposed.
- 2) An algorithm for finding the probability distribution of the candidate broadcast node (CBN) set is proposed based on the STM.
- 3) Based on the DCSMC model and the probability distribution of the CBN set, the existence conditions and the theoretical expressions for the limiting distribution of energy in energy buffers are derived.
- 4) Based on the limiting distributions of energy stored in buffers, the closed-form expressions are derived for system outage probability and throughput. Additionally, the derived analytical closed-forms and the theoretical

TABLE I: Comparison of references. Where N indicates that the technology is not adopted in the studied system, and Y indicates that the technology is adopted in the studied system.

Reference	EH buffer architecture	SSN	OR
[3], [4], [5]	HU	N	N
[6], [7], [8], [9], [10], [11], [12], [13]	HSU	N	N
[15], [16], [17], [18], [19], [20], [21]	HSU	Y	N
[23], [24], [25], [26], [27], [28], [29]	No EH	N	Y
Our work	HSU	Y	Y

analysis given are numerically validated.

The remainder of this paper is organized as follows. In section II, the system model and the proposed OR protocol is described. In section III, the limiting distributions of energy stored in buffers are shown. In section IV, the expressions are derived for system outage probability and throughput. Simulation and theory performance results are presented in Section V. Finally, the conclusion is presented in Section VI.

Notations : $A \sim \mathcal{CN}(0, \theta)$ indicates the random variable A follows the complex Gaussian distribution with mean 0 and variance θ . The absolute value of B is denoted by $|B|$. $\mathbb{E}[\cdot]$ denotes the expectation operator. $C_1 \cap C_2$ denotes that both the condition C_1 and the condition C_2 are satisfied, while $C_1 \cup C_2$ means that at least one of condition C_1 and condition C_2 is satisfied. $W(\cdot)$ is the Lambert W function. Boldface capital and lower-case letters stand for matrices and vectors, respectively. In addition, $\overline{C_1}$ represents the opposite of condition C_1 . $\|\cdot\|_2$ denotes the Euclidean norm of vector.

II. SYSTEM MODEL AND OR PROTOCOL

A. System Model

As illustrated in Fig. 1, the network considered in this paper consists of a source node S , a destination node D , and two DF relay nodes $R1$ and $R2$. In this network, all nodes operate in half duplex mode. The fixed power supply is assumed in both S and D , while $R1$ and $R2$ are equipped energy buffer shown in Fig. 2 and powered solely by the energy harvested from the ambience. More especially, in each time slot, there is only one activated node transmit signals to corresponding receiving nodes, while the inactive nodes keep silent or receive signals transmitted from the activated node. Additionally, the quasi-static Rayleigh fading channel model is assumed between all nodes, then, the channel coefficients within the i -th time slot between S and D , S and $R1$, S and $R2$, $R1$ and $R2$, $R1$ and D , and $R2$ and D can be denoted by $h_{SD}(i) \sim \mathcal{CN}(0, d_{SD}^{-\alpha})$, $h_{SR1}(i) \sim \mathcal{CN}(0, d_{SR1}^{-\alpha})$, $h_{SR2}(i) \sim \mathcal{CN}(0, d_{SR2}^{-\alpha})$, $h_{R1R2}(i) \sim \mathcal{CN}(0, d_{R1R2}^{-\alpha})$, $h_{R1D}(i) \sim \mathcal{CN}(0, d_{R1D}^{-\alpha})$ and $h_{R2D}(i) \sim \mathcal{CN}(0, d_{R2D}^{-\alpha})$, respectively, where d_{nm} denotes the distance between the node $n \in [S, R1, R2]$ and the node $m \in [R1, R2, D]$, and α is the path-loss parameter.

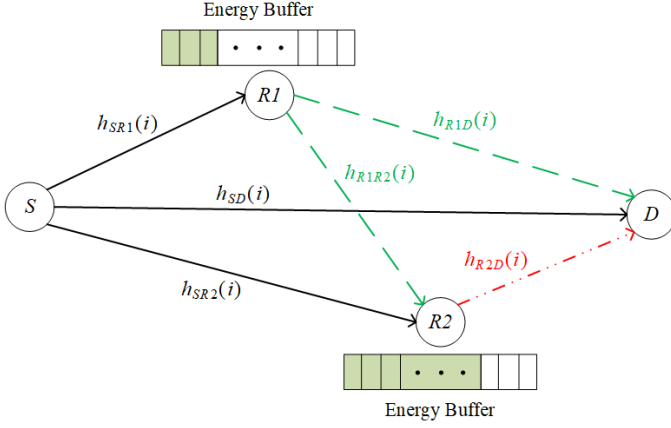


Fig. 1: System model.

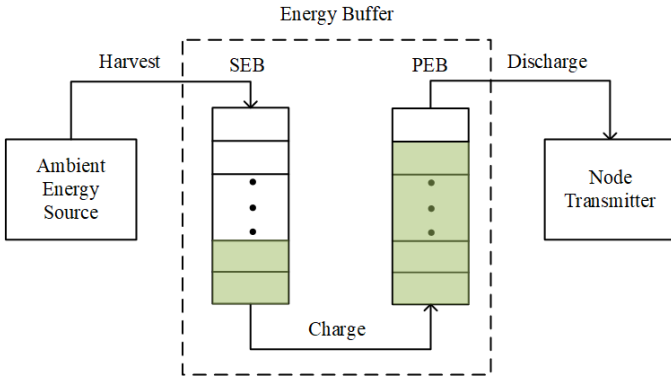


Fig. 2: HSU energy harvesting architecture.

The HSU energy harvesting architecture adopted by the energy buffers equipped by $R1$ and $R2$ is depicted in Fig. 2. It can be seen from Fig. 2 that the architecture mainly consists of an infinite-size primary energy buffer (PEB) and an infinite-size secondary energy buffer (SEB). Particularly, since the rechargeable energy storage devices are not able to discharge when they are being charged [30], [31], the PEB is utilized to power the node transmitter. In contrast, the harvested energy from the ambient energy source (e.g. the predictable solar energy [32]) needs to be stored in the SEB. In addition, for the sake of achieving the target that energy buffers equipped by $R1$ and $R2$ can charge and discharge simultaneously, it is assumed that the PEB may be charged instantaneously by the SEB at the end of one signal time slot. Moreover, the energy loss in the charging process between SEB and PEB and the energy loss in the discharging process between PEB and node transmitter are omitted. In [31], there is evidence to indicate that these assumptions are feasible.

In the proposed cooperative communication network, as shown in Fig. 1, the S may broadcast unit-energy signals $x_S(i)$ to $R1$, $R2$ and D at rate R_0 with the constant transmitting power P_S . The received signals $y_{SR1}(i)$, $y_{SR2}(i)$ and $y_{SD}(i)$ at $R1$, $R2$ and D in the i -th time slot can be represented by

$$y_{SR1}(i) = \sqrt{P_S} h_{SR1}(i) x_S(i) + n_{SR1}(i), \quad (1)$$

$$y_{SR2}(i) = \sqrt{P_S} h_{SR2}(i) x_S(i) + n_{SR2}(i), \quad (2)$$

$$y_{SD}(i) = \sqrt{P_S} h_{SD}(i) x_S(i) + n_{SD}(i), \quad (3)$$

where, $n_{SR1}(i)$, $n_{SR2}(i)$ and $n_{SD}(i) \sim \mathcal{CN}(0, N_0)$ denote the received additive white Gaussian noise (AWGN) at $R1$, $R2$ and D , respectively. Therefore, the instantaneous link signal to noise ratios (SNRs) $\gamma_{SR1}(i)$, $\gamma_{SR2}(i)$ and $\gamma_{SD}(i)$ at $R1$, $R2$ and D in the i -th time slot would be given as follows

$$\gamma_{SR1}(i) = \frac{P_S |h_{SR1}(i)|^2}{N_0}, \quad \gamma_{SR2}(i) = \frac{P_S |h_{SR2}(i)|^2}{N_0} \quad (4)$$

and
$$\gamma_{SD}(i) = \frac{P_S |h_{SD}(i)|^2}{N_0}.$$

Because of the DF mode, $R1$ decodes the received signals $x_S(i)$, re-encodes the information into unit-energy symbols $x_{R1}(i)$, and then broadcasts $x_{R1}(i)$ to $R2$ and D at rate R_0 with the constant power P_{R1} . Additionally, $R2$ processes the received signals in the same way as $R1$, and then broadcasts the unit-energy symbols $x_{R2}(i)$ to D at rate R_0 with the constant power P_{R2} . Next, the received signals $y_{R1R2}(i)$, $y_{R1D}(i)$ and $y_{R2D}(i)$ at $R2$ and D in the i -th time slot can be denoted by

$$y_{R1R2}(i) = \sqrt{P_{R1}} h_{R1R2}(i) x_{R1}(i) + n_{R1R2}(i), \quad (5)$$

$$y_{R1D}(i) = \sqrt{P_{R1}} h_{R1D}(i) x_{R1}(i) + n_{R1D}(i), \quad (6)$$

$$y_{R2D}(i) = \sqrt{P_{R2}} h_{R2D}(i) x_{R2}(i) + n_{R2D}(i), \quad (7)$$

where, $n_{R1R2}(i)$, $n_{R1D}(i)$ and $n_{R2D}(i) \sim \mathcal{CN}(0, N_0)$ denote the received AWGN at $R2$ and D , respectively. Similarly, the instantaneous link SNRs $\gamma_{R1R2}(i)$, $\gamma_{R1D}(i)$ and $\gamma_{R2D}(i)$ at $R2$ and D can be expressed as follows

$$\gamma_{R1R2}(i) = \frac{P_{R1} |h_{R1R2}(i)|^2}{N_0}, \quad \gamma_{R1D}(i) = \frac{P_{R1} |h_{R1D}(i)|^2}{N_0}$$

and
$$\gamma_{R2D}(i) = \frac{P_{R2} |h_{R2D}(i)|^2}{N_0}.$$
 (8)

The time slot diagram of the proposed cooperative communication network is shown in Fig. 3, where one time slot consists of pilot broadcasting sub-slot $t1$, packet broadcasting sub-slot $t2$ and positive acknowledgement (ACK) or negative acknowledgement (NACK) broadcasting sub-slot $t3$. Specifically, in sub-slot $t1$, nodes D , $R1$ and $R2$ need to broadcast the pilot signals orderly so that each node of this network can know the CSI between itself and other nodes. In sub-slot $t2$, using the OR protocol described in subsection II B, at most one node is selected to broadcast the packet while the other nodes keep silent. From Fig. 3 it can be seen that S , $R1$ and $R2$ are selected to broadcast the packet in time slot $T1$, time slot $T2$ and time slot $T3$ respectively. In sub-slot $t3$, nodes D , $R1$ and $R2$ broadcast ACK or NACK signals orderly. In particular, when the instantaneous link SNR at the receiving node is not less than the threshold $\Gamma_{th} = 2^{R_0} - 1$, ACK signals would be broadcasted by the receiving node as the sign of successful packet reception. Otherwise, NACK signals would be broadcasted by the receiving node as the sign of the packet reception failure.

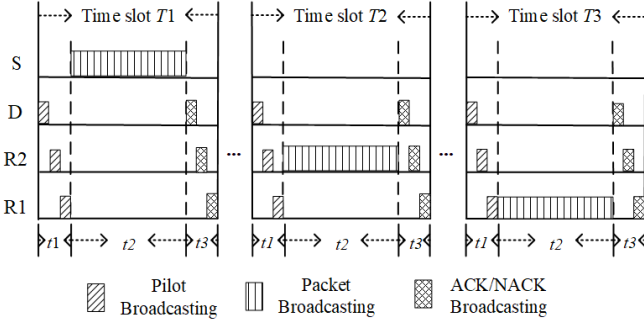


Fig. 3: System time slot diagram. Where one time slot consists of pilot broadcasting sub-slot t_1 , packet broadcasting sub-slot t_2 and positive acknowledgement (ACK) or negative acknowledgement (NACK) broadcasting sub-slot t_3 . Especially, in time slot T_1 , time slot T_2 and time slot T_3 , S , R_1 and R_2 are selected to broadcast the packet, respectively.

B. OR Protocol

In this section, the OR protocol is proposed. In the cooperative communication network shown in Fig. 1, it is first assumed that S always has the packet to be transmitted. Secondly, when transmitting the same packet to the same node, S has the highest transmission priority, R_2 has the second priority, and R_1 has the lowest priority. This is because S has fixed power support and can transmit the packet to R_1 , R_2 and D . Compared with S , EH-based R_1 can transmit the packet to R_2 and D , while EH-based R_2 can only transmit the packet to D . Third, as long as D receives the packet, S would transmit a new packet in the next time slot. In addition, the transmitting node which has the packet to be forwarded is named as CBN, and the node which can receive the packet transmitted by the CBN is named the neighbouring node of the CBN. The main procedures of OR protocol are divided into the following three steps:

- 1) : Determine the CBN set $\mathbf{S}(i) \in \{\mathbf{s}_1, \mathbf{s}_2, \mathbf{s}_3, \mathbf{s}_4\}$ in the current time slot, where $\mathbf{s}_1 = \{S\}$, $\mathbf{s}_2 = \{S, R_1\}$, $\mathbf{s}_3 = \{S, R_2\}$, $\mathbf{s}_4 = \{S, R_1, R_2\}$.
- 2) : According to the channel informations between nodes, the stored energy $B_1(i)$ of R_1 and the stored energy $B_2(i)$ of R_2 , in the current time slot, the broadcast node (BN) $BN(i) \in \{S, R_1, R_2, \simeq\}$ is selected from the CBN set $\mathbf{S}(i)$, where \simeq indicates that there is no node is selected to broadcast the packet in the current time slot.
- 3) : Determine the effective transmission and get CBN set $\mathbf{S}(i+1) \in \{\mathbf{s}_1, \mathbf{s}_2, \mathbf{s}_3, \mathbf{s}_4\}$ in the next time slot.

More especially, Table II describes the OR protocol in detail, where M_1 and M_2 denote the energy consumed by R_1 and R_2 to broadcast the packet in one time slot, respectively. Moreover, M_1 and M_2 are numerically equal to P_{R1} and P_{R2} , respectively.

III. LIMITING DISTRIBUTION OF ENERGY

This section is concerned with the limiting distributions of stored energy in the infinite-size energy buffers with HSU architecture. Specially, it is assumed that $X_1(i)$ and $X_2(i)$ are the energy harvested by R_1 and R_2 from the surrounding

environment in one time slot, respectively. Moreover, $X_1(i)$ and $X_2(i)$ are exponentially distributed random variables (as in both [30] and [31]) with means $\mathbb{E}[X_1(i)] = 1/\lambda_1$ and $\mathbb{E}[X_2(i)] = 1/\lambda_2$, respectively. So that the probability density function (PDF) of $X_1(i)$ and $X_2(i)$ can be expressed as follows

$$f_{X_j}(x) = \lambda_j e^{-\lambda_j x}, \quad x > 0, j = 1, 2. \quad (9)$$

A. Limiting Distribution of R_2 Energy

Using the DCSMC on the continuous state space $[0, \infty)$, the dynamic process $B_2(i)$ of the energy storage in the infinite-size energy buffer of R_2 can be given as follows

$$\begin{aligned} B_2(i+1) &= B_2(i) + X_2(i), & \mathbb{P}_{21} \\ B_2(i+1) &= B_2(i) - M_2 + X_2(i), & \mathbb{P}_{22} \end{aligned} \quad (10)$$

where \mathbb{P}_{21} and \mathbb{P}_{22} are the conditions required for the storage equations in Eq. (10) to hold according to the OR protocol shown in Table II. And \mathbb{P}_{21} and \mathbb{P}_{22} can be expressed as follows

$$\begin{aligned} \mathbb{P}_{21} : & \left((\mathbf{S}(i) = \mathbf{s}_3) \cup (\mathbf{S}(i) = \mathbf{s}_4) \right) \cap \left[C_1(i) \cup \langle \overline{C_1}(i) \right. \\ & \cap (B_2(i) \geq M_2) \cap (\gamma_{R2D}(i) < \Gamma_{th}) \rangle \cup \langle \overline{C_1}(i) \\ & \left. \cap (B_2(i) < M_2) \right] \cup (\mathbf{S}(i) = \mathbf{s}_1) \cup (\mathbf{S}(i) = \mathbf{s}_2), \end{aligned} \quad (11)$$

$$\mathbb{P}_{22} : \left((\mathbf{S}(i) = \mathbf{s}_3) \cup (\mathbf{S}(i) = \mathbf{s}_4) \right) \cap C_9(i). \quad (12)$$

where $C_1(i)$ and $C_9(i)$ are given in Table II.

Let p_1 , p_2 , p_3 and p_4 denote the probabilities $\Pr\{\mathbf{S}(i) = \mathbf{s}_1\}$, $\Pr\{\mathbf{S}(i) = \mathbf{s}_2\}$, $\Pr\{\mathbf{S}(i) = \mathbf{s}_3\}$ and $\Pr\{\mathbf{S}(i) = \mathbf{s}_4\}$ in the case of stable energy buffers, respectively, and the values of these probabilities can be obtained in Alg. 1 which is introduced in subsection III C. Then, define $\Omega_{SD} = \frac{d_{SD}^\alpha N_0}{P_S}$, $\Omega_{SR2} = \frac{d_{SR2}^\alpha N_0}{P_S}$, $\Omega_{SR1} = \frac{d_{SR1}^\alpha N_0}{P_S}$, $\Omega_{R1D} = \frac{d_{R1D}^\alpha N_0}{M_1}$, $\Omega_{R1R2} = \frac{d_{R1R2}^\alpha N_0}{M_1}$ and $\Omega_{R2D} = \frac{d_{R2D}^\alpha N_0}{M_2}$. Furthermore, let ψ_2 denote the energy buffer stabilization parameter for the energy storage process $B_2(i)$ in Eq. (10), which can be expressed as follows

$$\begin{aligned} \psi_2 &= \lambda_2 M_2 [(p_3 + p_4) (1 - e^{-\Omega_{SD} \Gamma_{th}}) e^{-\Omega_{R2D} \Gamma_{th}}] \\ &= \frac{M_2 [(p_3 + p_4) (1 - e^{-\Omega_{SD} \Gamma_{th}}) e^{-\Omega_{R2D} \Gamma_{th}}]}{\mathbb{E}[X_2(i)]}. \end{aligned} \quad (13)$$

Theorem 1: If $\psi_2 \leq 1$, the energy storage process $B_2(i)$ in Eq. (10) will not have a stationary distribution. Moreover, after a finite number of time slots, $B_2(i) > M_2$ almost always hold.

Proof 1: The proof is presented in Appendix A.

Theorem 2: For the storage process $B_2(i)$ in Eq. (10), the limiting energy distribution exists with $\psi_2 > 1$. Furthermore, the limiting PDF of the energy buffer state at R_2 can be given by

$$g_2(x) = \begin{cases} \frac{1}{M_2} (1 - e^{Q_2 x}), & 0 \leq x < M_2 \\ \frac{1}{M_2} \frac{-Q_2 e^{Q_2 x}}{(b_2 \lambda_2 + Q_2)}, & x \geq M_2 \end{cases} \quad (14)$$

TABLE II: The OR Protocol. In the current time slot, the protocol determines the broadcast node (BN) $BN(i)$ and effective transmission according to the known candidate broadcast node (CBN) set $\mathbf{S}(i)$ and the known conditions (energy information stored by relay nodes and channel information), and further obtains the CBN set $\mathbf{S}(i+1)$ of the next time slot.

CBN set $\mathbf{S}(i)$	Conditions	BN $BN(i)$	Effective transmission	CBN set $\mathbf{S}(i+1)$
$\mathbf{s}_1 = \{\mathbf{S}\}$	$C_1(i) : \gamma_{SD}(i) \geq \Gamma_{th}$	\mathbf{S}	$\mathbf{S} \rightarrow \mathbf{D}$	$\mathbf{s}_1 = \{\mathbf{S}\}$
	$C_2(i) : \gamma_{SD}(i) < \Gamma_{th} \cap \gamma_{SR1}(i) \geq \Gamma_{th} \cap \gamma_{SR2}(i) < \Gamma_{th}$		$\mathbf{S} \rightarrow \mathbf{R1}$	$\mathbf{s}_2 = \{\mathbf{S}, \mathbf{R1}\}$
	$C_3(i) : \gamma_{SD}(i) < \Gamma_{th} \cap \gamma_{SR1}(i) < \Gamma_{th} \cap \gamma_{SR2}(i) \geq \Gamma_{th}$		$\mathbf{S} \rightarrow \mathbf{R2}$	$\mathbf{s}_3 = \{\mathbf{S}, \mathbf{R2}\}$
	$C_4(i) : \gamma_{SD}(i) < \Gamma_{th} \cap \gamma_{SR1}(i) \geq \Gamma_{th} \cap \gamma_{SR2}(i) \geq \Gamma_{th}$		$\mathbf{S} \rightarrow \mathbf{R1}, \mathbf{R2}$	$\mathbf{s}_4 = \{\mathbf{S}, \mathbf{R1}, \mathbf{R2}\}$
	others	\simeq	\simeq	$\mathbf{s}_1 = \{\mathbf{S}\}$
$\mathbf{s}_2 = \{\mathbf{S}, \mathbf{R1}\}$	$C_1(i) : \gamma_{SD}(i) \geq \Gamma_{th}$	\mathbf{S}	$\mathbf{S} \rightarrow \mathbf{D}$	$\mathbf{s}_1 = \{\mathbf{S}\}$
	$C_5(i) : \gamma_{SD}(i) < \Gamma_{th} \cap B_1(i) \geq M_1 \cap \gamma_{R1D}(i) \geq \Gamma_{th}$	$\mathbf{R1}$	$\mathbf{R1} \rightarrow \mathbf{D}$	
	$C_6(i) : \gamma_{SD}(i) < \Gamma_{th} \cap B_1(i) \geq M_1 \cap \gamma_{R1D}(i) < \Gamma_{th}$ $\cap \gamma_{SR2}(i) \geq \Gamma_{th}$	\mathbf{S}	$\mathbf{S} \rightarrow \mathbf{R2}$	$\mathbf{s}_4 = \{\mathbf{S}, \mathbf{R1}, \mathbf{R2}\}$
	$C_7(i) : \gamma_{SD}(i) < \Gamma_{th} \cap B_1(i) < M_1 \cap \gamma_{SR2}(i) \geq \Gamma_{th}$			
	$C_8(i) : \gamma_{SD}(i) < \Gamma_{th} \cap B_1(i) \geq M_1 \cap \gamma_{R1D}(i) < \Gamma_{th}$ $\cap \gamma_{SR2}(i) < \Gamma_{th} \cap \gamma_{R1R2}(i) \geq \Gamma_{th}$	$\mathbf{R1}$	$\mathbf{R1} \rightarrow \mathbf{R2}$	
	others	\simeq	\simeq	$\mathbf{s}_2 = \{\mathbf{S}, \mathbf{R1}\}$
$\mathbf{s}_3 = \{\mathbf{S}, \mathbf{R2}\}$	$C_1(i) : \gamma_{SD}(i) \geq \Gamma_{th}$	\mathbf{S}	$\mathbf{S} \rightarrow \mathbf{D}$	$\mathbf{s}_1 = \{\mathbf{S}\}$
	$C_9(i) : \gamma_{SD}(i) < \Gamma_{th} \cap B_2(i) \geq M_2 \cap \gamma_{R2D}(i) \geq \Gamma_{th}$	$\mathbf{R2}$	$\mathbf{R2} \rightarrow \mathbf{D}$	
	others	\simeq	\simeq	$\mathbf{s}_3 = \{\mathbf{S}, \mathbf{R2}\}$
$\mathbf{s}_4 = \{\mathbf{S}, \mathbf{R1}, \mathbf{R2}\}$	$C_1(i) : \gamma_{SD}(i) \geq \Gamma_{th}$	\mathbf{S}	$\mathbf{S} \rightarrow \mathbf{D}$	$\mathbf{s}_1 = \{\mathbf{S}\}$
	$C_9(i) : \gamma_{SD}(i) < \Gamma_{th} \cap B_2(i) \geq M_2 \cap \gamma_{R2D}(i) \geq \Gamma_{th}$	$\mathbf{R2}$	$\mathbf{R2} \rightarrow \mathbf{D}$	
	$C_{10}(i) : \gamma_{SD}(i) < \Gamma_{th} \cap B_2(i) \geq M_2 \cap \gamma_{R2D}(i) < \Gamma_{th}$ $\cap B_1(i) \geq M_1 \cap \gamma_{R1D}(i) \geq \Gamma_{th}$	$\mathbf{R1}$	$\mathbf{R1} \rightarrow \mathbf{D}$	
	$C_{11}(i) : \gamma_{SD}(i) < \Gamma_{th} \cap B_2(i) < M_2 \cap B_1(i) \geq M_1$ $\cap \gamma_{R1D}(i) \geq \Gamma_{th}$			
	others	\simeq	\simeq	$\mathbf{s}_4 = \{\mathbf{S}, \mathbf{R1}, \mathbf{R2}\}$

where,

$$b_2 = [(p_3 + p_4) (1 - e^{-\Omega_{SD}\Gamma_{th}}) e^{-\Omega_{R2D}\Gamma_{th}}], \quad (15)$$

and $Q_2 = \frac{-W(-b_2\lambda_2 M_2 e^{-b_2\lambda_2 M_2})}{M_2} - b_2\lambda_2 < 0$, satisfying $b_2\lambda_2 e^{Q_2 M_2} = b_2\lambda_2 + Q_2$. Furthermore, the probabilities $\Pr\{B_2(i) \geq M_R\}$ and $\Pr\{B_2(i) < M_R\}$ may be written as follows

$$\begin{aligned} \Pr\{B_2(i) \geq M_2\} &= \int_{x=M_2}^{\infty} \frac{-Q_2 e^{Q_2 x}}{M_2 (b_2\lambda_2 + Q_2)} dx \\ &= \frac{e^{Q_2 M_2}}{M_2 (b_2\lambda_2 + Q_2)} = \frac{1}{M_2 b_2\lambda_2}, \end{aligned} \quad (16)$$

$$\Pr\{B_2(i) < M_2\} = 1 - \frac{1}{M_2 b_2\lambda_2}. \quad (17)$$

Proof 2: The proof is presented in Appendix B.

B. Limiting Distribution of R1 Energy

Similarly, Let $B_1(i)$ denotes the dynamic process of the energy storage in the infinite-size energy buffer of relay R1 using the DSCMC on a continuous state space $[0, \infty)$, which can be given by the storage equation as follows

$$\begin{aligned} B_1(i+1) &= B_1(i) + X_1(i), \quad \mathbb{P}_{11} \\ B_1(i+1) &= B_1(i) - M_1 + X_1(i), \quad \mathbb{P}_{12} \end{aligned} \quad (18)$$

Where \mathbb{P}_{11} and \mathbb{P}_{12} are the conditions required for above OR protocol based storage equations to hold, and they are shown in Eq. (19) and Eq. (20), respectively.

$$\begin{aligned} \mathbb{P}_{12} : & \left[(\mathbf{S}(i) = \mathbf{s}_2) \cap \langle C_5(i) \cup C_8(i) \rangle \right] \\ & \cup \left[(\mathbf{S}(i) = \mathbf{s}_4) \cap \langle C_{10}(i) \cup C_{11}(i) \rangle \right]. \end{aligned} \quad (20)$$

where $C_1(i)$, $C_5(i)$, $C_8(i)$, $C_9(i)$, $C_{10}(i)$ and $C_{11}(i)$ are given in Table II.

The energy buffer stabilization parameter ψ_2 for the energy storage process $B_2(i)$ of Eq. (18) can be expressed as follows

$$\begin{aligned} \psi_1 &= \lambda_1 M_1 (1 - e^{-\Omega_{SD}\Gamma_{th}}) \left[p_2 e^{-\Omega_{R1D}\Gamma_{th}} \right. \\ &+ p_2 (1 - e^{-\Omega_{R1D}\Gamma_{th}}) (1 - e^{-\Omega_{SR2}\Gamma_{th}}) e^{-\Omega_{R1R2}\Gamma_{th}} \\ &+ p_4 e^{-\Omega_{R1D}\Gamma_{th}} \left(1 - \frac{e^{-\Omega_{R2D}\Gamma_{th}}}{M_2 b_2\lambda_2} \right) \left. \right]. \end{aligned} \quad (21)$$

Theorem 3: Similarly, for the energy storage process $B_1(i)$ in Eq. (18), the stationary distribution does not exist when $\psi_1 \leq 1$, and there is always M_1 amount of energy available in the buffer.

Proof 3: The proof of theorem 3 only needs to replace \mathbb{P}_{21} and \mathbb{P}_{22} in Eq. (53) with \mathbb{P}_{11} and \mathbb{P}_{12} , respectively, and the rest is the same as the proof process of theorem 1.

$$\begin{aligned}
\mathbb{P}_{11} : & (\mathbf{S}(i) = \mathbf{s}_1) \cup (\mathbf{S}(i) = \mathbf{s}_3) \cup (\mathbf{S}(i) = \mathbf{s}_2) \cap \left\{ C_1(i) \cup \left\langle \overline{C_1}(i) \cap (B_1(i) \geq M_1) \cap (\gamma_{R1D}(i) < \Gamma_{th}) \right\rangle \right. \\
& \cap \left[\left\langle (\gamma_{SR2}(i) < \Gamma_{th}) \cap (\gamma_{R1R2}(i) < \Gamma_{th}) \right\rangle \cup (\gamma_{SR2}(i) \geq \Gamma_{th}) \right] \cup \left\langle \overline{C_1}(i) \cap (B_1(i) < M_1) \right\rangle \left. \right\} \\
& \cup (\mathbf{S}(i) = \mathbf{s}_4) \cap \left\{ C_1(i) \cup C_9(i) \cup \overline{C_1}(i) \cap \left[\left\langle (B_2(i) \geq M_2) \cap (\gamma_{R2D}(i) < \Gamma_{th}) \right\rangle \cup (B_2(i) < M_2) \right] \right. \\
& \cap \left[\left\langle (B_1(i) \geq M_1) \cap (\gamma_{R1D}(i) < \Gamma_{th}) \right\rangle \cup (B_1(i) < M_1) \right] \left. \right\}
\end{aligned} \tag{19}$$

Theorem 4: When, $\psi_1 > 1$, the limiting distribution of $B_1(i)$ exists and the limiting PDF $g_1(x)$ of $B_1(i)$ can be given by

$$g_1(x) = \begin{cases} \frac{1}{M_1} (1 - e^{Q_1 x}), & 0 \leq x < M_1 \\ \frac{1}{M_1} \frac{-Q_1 e^{Q_1 x}}{(b_1 \lambda_1 + Q_1)}, & x \geq M_1. \end{cases} \tag{22}$$

where, b_1 is given as follows

$$\begin{aligned}
b_1 = & (1 - e^{-\Omega_{SD}\Gamma_{th}}) \left[p_2 e^{-\Omega_{R1D}\Gamma_{th}} \right. \\
& + p_2 (1 - e^{-\Omega_{R1D}\Gamma_{th}}) (1 - e^{-\Omega_{SR2}\Gamma_{th}}) e^{-\Omega_{R1R2}\Gamma_{th}} \\
& \left. + p_4 e^{-\Omega_{R1D}\Gamma_{th}} \left(1 - \frac{e^{-\Omega_{R2D}\Gamma_{th}}}{M_2 b_2 \lambda_2} \right) \right],
\end{aligned} \tag{23}$$

and $Q_1 = \frac{-W(-b_1 \lambda_1 M_1 e^{-b_1 \lambda_1 M_1})}{M_1} - b_1 \lambda_1 < 0$, satisfying $b_1 \lambda_1 e^{Q_1 M_1} = b_1 \lambda_1 + Q_1$. In addition, the probabilities $\Pr\{B_1(i) \geq M_1\}$ and $\Pr\{B_1(i) < M_1\}$ may be written as follows

$$\begin{aligned}
\Pr\{B_1(i) \geq M_1\} &= \int_{x=M_1}^{\infty} \frac{-Q_1 e^{Q_1 x}}{M_1 (b_1 \lambda_1 + Q_1)} dx \\
&= \frac{e^{Q_1 M_1}}{M_1 (b_1 \lambda_1 + Q_1)} = \frac{1}{M_1 b_1 \lambda_1},
\end{aligned} \tag{24}$$

$$\Pr\{B_1(i) < M_1\} = 1 - \frac{1}{M_1 b_1 \lambda_1}. \tag{25}$$

Proof 4: The proof is presented in Appendix C.

C. The Probability Distribution of CBN Set \mathbf{S} in the Case of Stable Energy Buffer

The previous theorem 2 and theorem 4 illustrate that after some time slots, the energy buffers in $R1$ and $R2$ will reach their own stable states under the condition of $\psi_1 > 1$ and $\psi_2 > 1$. Moreover, when the energy buffers in $R1$ and $R2$ reach their own stable states, the probability distribution $\mathbf{p} = [p_1, p_2, p_3, p_4]$ of CBN Set \mathbf{S} may be obtained by STM, which is expressed as follows

$$\mathbf{p}(i+1) = \mathbf{p}(i)\mathbf{T}(i), \tag{26}$$

where $\mathbf{p}(i) = [p_1(i), p_2(i), p_3(i), p_4(i)]$ denotes the values of \mathbf{p} in the i -th time slot, $\mathbf{p}(i+1) = [p_1(i+1), p_2(i+1), p_3(i+1), p_4(i+1)]$ denotes the values of \mathbf{p} in the $(i+1)$ -th time slot, and $\mathbf{T}(i)$ is the STM of these probabilities from $\mathbf{p}(i)$ to

$\mathbf{p}(i+1)$. Furthermore, according to table II, the STM $\mathbf{T}(i)$ can be constructed as follows

$$\mathbf{T}(i) = \begin{bmatrix} p_{s_1 s_1}(i) & p_{s_1 s_2}(i) & p_{s_1 s_3}(i) & p_{s_1 s_4}(i) \\ p_{s_2 s_1}(i) & p_{s_2 s_2}(i) & p_{s_2 s_3}(i) & p_{s_2 s_4}(i) \\ p_{s_3 s_1}(i) & p_{s_3 s_2}(i) & p_{s_3 s_3}(i) & p_{s_3 s_4}(i) \\ p_{s_4 s_1}(i) & p_{s_4 s_2}(i) & p_{s_4 s_3}(i) & p_{s_4 s_4}(i) \end{bmatrix}, \tag{27}$$

where, the element $p_{IJ}(k)$ ($I, J \in \{s_1, s_2, s_3, s_4\}$) denotes the probability that the CBN set $\mathbf{S}(i)$ changes from I in the i -th time slot to J in the $(i+1)$ -th time slot, satisfying $\sum_{J \in \{s_1, s_2, s_3, s_4\}} p_{IJ}(i) = 1$. Furthermore, according to the variables $\gamma_{SD}, \gamma_{SR1}, \gamma_{SR2}, \gamma_{R1D}, \gamma_{R1R2}, \gamma_{R2D}$, $\Pr\{B_2(i) \geq M_2\}$, $\Pr\{B_1(i) \geq M_1\}$, and the OR protocol shown in Table II, $p_{IJ}(i)$ may be obtained as follows

$$\begin{aligned}
p_{s_1 s_1}(i) &= \Pr\{\gamma_{SD}(i) < \Gamma_{th}, \gamma_{SR1}(i) < \Gamma_{th}, \gamma_{SR2}(i) < \Gamma_{th}\} \\
&+ \Pr\{C_1(i)\} \\
&= (1 - e^{-\Omega_{SD}\Gamma_{th}}) (1 - e^{-\Omega_{SR1}\Gamma_{th}}) (1 - e^{-\Omega_{SR2}\Gamma_{th}}) \\
&+ e^{-\Omega_{SD}\Gamma_{th}},
\end{aligned} \tag{28}$$

$$\begin{aligned}
p_{s_1 s_2}(i) &= \Pr\{C_2(i)\} \\
&= (1 - e^{-\Omega_{SD}\Gamma_{th}}) e^{-\Omega_{SR1}\Gamma_{th}} (1 - e^{-\Omega_{SR2}\Gamma_{th}}),
\end{aligned} \tag{29}$$

$$\begin{aligned}
p_{s_1 s_3}(i) &= \Pr\{C_3(i)\} \\
&= (1 - e^{-\Omega_{SD}\Gamma_{th}}) (1 - e^{-\Omega_{SR1}\Gamma_{th}}) e^{-\Omega_{SR2}\Gamma_{th}},
\end{aligned} \tag{30}$$

$$\begin{aligned}
p_{s_1 s_4}(i) &= \Pr\{C_4(i)\} \\
&= (1 - e^{-\Omega_{SD}\Gamma_{th}}) e^{-\Omega_{SR1}\Gamma_{th}} e^{-\Omega_{SR2}\Gamma_{th}},
\end{aligned} \tag{31}$$

and,

$$\begin{aligned}
p_{s_2 s_1}(i) &= \Pr\{C_1(i)\} + \Pr\{C_5(i)\} \\
&= e^{-\Omega_{SD}\Gamma_{th}} + \frac{(1 - e^{-\Omega_{SD}\Gamma_{th}}) e^{-\Omega_{R1D}\Gamma_{th}}}{b_1(i) \lambda_1 M_1},
\end{aligned} \tag{32}$$

$$\begin{aligned}
p_{s_2 s_2}(i) &= \Pr\{\overline{C_1}(i), B_1(i) \geq M_1, \gamma_{R1D}(i) < \Gamma_{th}, \\
&\gamma_{SR2}(i) < \Gamma_{th}, \gamma_{R1R2}(i) < \Gamma_{th}\} \\
&+ \Pr\{\overline{C_1}(i), B_1(i) < M_1, \gamma_{SR2}(i) < \Gamma_{th}\} \\
&= (1 - e^{-\Omega_{SD}\Gamma_{th}}) (1 - e^{-\Omega_{SR2}\Gamma_{th}}) \\
&\times \left[\frac{(1 - e^{-\Omega_{R1D}\Gamma_{th}}) (1 - e^{-\Omega_{R1R2}\Gamma_{th}})}{b_1(i) \lambda_1 M_1} \right. \\
&\left. + \left(1 - \frac{1}{b_1(i) \lambda_1 M_1} \right) \right],
\end{aligned} \tag{33}$$

$$\begin{aligned}
p_{s_2s_4}(i) &= \Pr\{C_6(i)\} + \Pr\{C_7(i)\} + \Pr\{C_8(i)\} \\
&= (1 - e^{-\Omega_{SD}\Gamma_{th}}) \left[e^{-\Omega_{SR2}\Gamma_{th}} \left(1 - \frac{e^{-\Omega_{R1D}\Gamma_{th}}}{b_1(i)\lambda_1 M_1} \right) \right. \\
&\quad \left. + \frac{(1 - e^{-\Omega_{R1D}\Gamma_{th}})(1 - e^{-\Omega_{SR2}\Gamma_{th}})e^{-\Omega_{R1R2}\Gamma_{th}}}{b_1(i)\lambda_1 M_1} \right], \quad (34)
\end{aligned}$$

$$p_{s_2s_3}(i) = 0, \quad (35)$$

and,

$$\begin{aligned}
p_{s_3s_1}(i) &= \Pr\{C_1(i)\} + \Pr\{C_9(i)\} \\
&= e^{-\Omega_{SD}\Gamma_{th}} + \frac{(1 - e^{-\Omega_{SD}\Gamma_{th}})e^{-\Omega_{R2D}\Gamma_{th}}}{b_2(i)\lambda_2 M_2}, \quad (36)
\end{aligned}$$

$$\begin{aligned}
p_{s_3s_3}(i) &= \Pr\{\overline{C_1}(i), B_2(i) < M_2\} \\
&\quad + \Pr\{\overline{C_1}(i), B_2(i) \geq M_2, \gamma_{R2D}(i) < \Gamma_{th}\} \\
&= (1 - e^{-\Omega_{SD}\Gamma_{th}}) \left(1 - \frac{e^{-\Omega_{R2D}\Gamma_{th}}}{b_2(i)\lambda_2 M_2} \right), \quad (37)
\end{aligned}$$

$$p_{s_3s_2}(i) = p_{s_3s_4}(i) = 0, \quad (38)$$

and,

$$\begin{aligned}
p_{s_4s_1}(i) &= \Pr\{C_1(i)\} + \Pr\{C_9(i)\} + \Pr\{C_{10}(i)\} \\
&\quad + \Pr\{C_{11}(i)\} \\
&= e^{-\Omega_{SD}\Gamma_{th}} + \frac{(1 - e^{-\Omega_{SD}\Gamma_{th}})e^{-\Omega_{R2D}\Gamma_{th}}}{b_2(i)\lambda_2 M_2} \\
&\quad + \frac{(1 - e^{-\Omega_{SD}\Gamma_{th}})e^{-\Omega_{R1D}\Gamma_{th}}}{b_1(i)\lambda_1 M_1} \\
&\quad \times \left(1 - \frac{e^{-\Omega_{R2D}\Gamma_{th}}}{b_2(i)\lambda_2 M_2} \right), \quad (39)
\end{aligned}$$

$$\begin{aligned}
p_{s_4s_4}(i) &= \Pr\{\overline{C_1}(i), B_2(i) \geq M_2, \gamma_{R2D}(i) < \Gamma_{th}, \\
&\quad B_1(i) \geq M_1, \gamma_{R1D}(i) < \Gamma_{th}\} \\
&\quad + \Pr\{\overline{C_1}(i), B_2(i) \geq M_2, \gamma_{R2D}(i) < \Gamma_{th}, \\
&\quad B_1(i) < M_1, \} \\
&\quad + \Pr\{\overline{C_1}(i), B_2(i) < M_2, B_1(i) \geq M_1, \\
&\quad \gamma_{R1D}(i) < \Gamma_{th}\} \\
&\quad + \Pr\{\overline{C_1}(i), B_2(i) < M_2, B_1(i) < M_1\} \\
&= 1 - p_{s_4s_1}(i), \quad (40)
\end{aligned}$$

$$p_{s_4s_2}(i) = p_{s_4s_3}(i) = 0, \quad (41)$$

where $C_l(i) (l \in \{1, 2, \dots, 11\})$ is given in Table II, $b_2(i)$ and $b_1(i)$ are given by

$$\begin{aligned}
b_2(i) &= [(p_3(i) + p_4(i))(1 - e^{-\Omega_{SD}\Gamma_{th}})e^{-\Omega_{R2D}\Gamma_{th}}], \quad (42) \\
b_1(i) &= (1 - e^{-\Omega_{SD}\Gamma_{th}}) \left[p_2(i)e^{-\Omega_{R1D}\Gamma_{th}} \right. \\
&\quad + p_2(i)(1 - e^{-\Omega_{R1D}\Gamma_{th}})(1 - e^{-\Omega_{SR2}\Gamma_{th}})e^{-\Omega_{R1R2}\Gamma_{th}} \\
&\quad \left. + p_4(i)e^{-\Omega_{R1D}\Gamma_{th}} \left(1 - \frac{e^{-\Omega_{R2D}\Gamma_{th}}}{M_2 b_2(i)\lambda_2} \right) \right]. \quad (43)
\end{aligned}$$

The detailed process for obtaining probability distribution \mathbf{p} is shown in Alg. 1. Specifically, in line 5, the judgment condition ($\mathbf{p}_{j_1}(i) \leq 0 \mid \mathbf{T}_{j_1, j_2}(i) < 0$) indicates that there are

non-positive elements in $\mathbf{p}(i)$ or $\mathbf{T}(i)$, which is not desirable, so the update process needs to be terminated. Moreover, in line 8, ($\|\mathbf{p}(i) - \mathbf{p}(i+1)\|_2 < 10^{-7}$) indicates that the update error is small enough and the update process has converged. Therefore, the update process can be terminated.

Algorithm 1 Probability Distribution \mathbf{p} of CBN Set \mathbf{S} based on STM

Input: $\Omega_{SD}, \Omega_{SR1}, \Omega_{SR2}, \Omega_{R1D}, \Omega_{R1R2}, \Omega_{R2D}, \Gamma_{th}, \lambda_1, \lambda_2, M_1, M_2$.

- 1: Initialize $i = 0, k = 0, j_1$ and $j_2 \in \{1, 2, 3, 4\}$, $\mathbf{p}(0) = [p_1(0), p_2(0), p_3(0), p_4(0)] = [\frac{1}{4}, \frac{1}{4}, \frac{1}{4}, \frac{1}{4}]$.
- 2: **while** 1 **do**
- 3: Calculate $\mathbf{T}(i)$ according to $\mathbf{p}(i)$ and equations from Eq. (28) to Eq. (43),
- 4: $\mathbf{p}(i+1) = \mathbf{p}(i)\mathbf{T}(i)$,
- 5: **if** ($\mathbf{p}_{j_1}(i) \leq 0 \mid \mathbf{T}_{j_1, j_2}(i) < 0$) **then**
- 6: $k = i - 1$,
- 7: **break**,
- 8: **else if** ($\|\mathbf{p}(i) - \mathbf{p}(i+1)\|_2 < 10^{-7}$) **then**
- 9: $k = i$,
- 10: **break**,
- 11: **else**
- 12: $i = i + 1$,
- 13: **end if**
- 14: **end while**

Output: Probability Distribution $\mathbf{p}(k)$.

IV. ANALYSIS OF OUTAGE PROBABILITY AND THROUGHPUT

This section is concerned with the system performance metrics, including outage probability and throughput, when the states of system energy buffers are stable. Specifically, with the OR protocol shown in Table II, the system is in outage if the destination node D fails to receive the packet from the transmitting node $S, R1$ or $R2$. Furthermore, the system outage probability OP is defined as follows

$$OP = 1 - (P_{s_1} + P_{s_2} + P_{s_3} + P_{s_4}), \quad (44)$$

where, $P_{s_1}, P_{s_2}, P_{s_3}$ and P_{s_4} represent the probability that the destination node D successfully receive the packet in the case of $\mathbf{S}(i) = \mathbf{s}_1, \mathbf{S}(i) = \mathbf{s}_2, \mathbf{S}(i) = \mathbf{s}_3, \mathbf{S}(i) = \mathbf{s}_4$, respectively. According to Table II, they are expressed as follows

$$\begin{aligned}
P_{s_1} &= \Pr\{\mathbf{S}(i) = \mathbf{s}_1\} \Pr\{C_1(i)\} \\
&= p_1 e^{-\Omega_{SD}\Gamma_{th}}, \quad (45)
\end{aligned}$$

$$\begin{aligned}
P_{s_2} &= \Pr\{\mathbf{S}(i) = \mathbf{s}_2\} (\Pr\{C_1(i)\} + \Pr\{C_5(i)\}) \\
&= p_2 \left[e^{-\Omega_{SD}\Gamma_{th}} + \frac{(1 - e^{-\Omega_{SD}\Gamma_{th}})e^{-\Omega_{R1D}\Gamma_{th}}}{b_1\lambda_1 M_1} \right], \quad (46)
\end{aligned}$$

$$\begin{aligned}
P_{s_3} &= \Pr\{\mathbf{S}(i) = \mathbf{s}_3\} (\Pr\{C_1(i)\} + \Pr\{C_9(i)\}) \\
&= p_3 \left[e^{-\Omega_{SD}\Gamma_{th}} + \frac{(1 - e^{-\Omega_{SD}\Gamma_{th}})e^{-\Omega_{R2D}\Gamma_{th}}}{b_2\lambda_2 M_2} \right], \quad (47)
\end{aligned}$$

$$\begin{aligned}
P_{s_4} &= \Pr\{\mathbf{S}(i) = \mathbf{s}_4\} \left(\Pr\{C_1(i)\} + \Pr\{C_9(i)\} \right. \\
&\quad \left. + \Pr\{C_{10}(i)\} + \Pr\{C_{11}(i)\} \right) \\
&= p_4 \left[e^{-\Omega_{SD}\Gamma_{th}} + \frac{(1 - e^{-\Omega_{SD}\Gamma_{th}}) e^{-\Omega_{R2D}\Gamma_{th}}}{b_2 \lambda_2 M_2} + \right. \\
&\quad \left. \frac{(1 - e^{-\Omega_{SD}\Gamma_{th}}) e^{-\Omega_{R1D}\Gamma_{th}}}{b_1 \lambda_1 M_1} \left(1 - \frac{e^{-\Omega_{R2D}\Gamma_{th}}}{b_2 \lambda_2 M_2} \right) \right], \quad (48)
\end{aligned}$$

where $C_1(i)$, $C_5(i)$, $C_9(i)$, $C_{10}(i)$ and $C_{11}(i)$ are given in Table II. According to b_2 in Eq. (15) and the equations from Eq. (44) to Eq. (48), it can be known that the system outage probability OP in Eq. (44) can be rewritten as follows

$$\begin{aligned}
OP &= 1 - \left\{ e^{-\Omega_{SD}\Gamma_{th}} + \frac{1}{\lambda_2 M_2} \right. \\
&\quad \left. + \left[p_2 + p_4 \left(1 - \frac{e^{-\Omega_{R2D}\Gamma_{th}}}{b_2 \lambda_2 M_2} \right) \right] \right. \\
&\quad \left. \times \frac{(1 - e^{-\Omega_{SD}\Gamma_{th}}) e^{-\Omega_{R1D}\Gamma_{th}}}{b_1 \lambda_1 M_1} \right\}. \quad (49)
\end{aligned}$$

Furthermore, considering that the system needs to consume sub slots t_1 and t_2 for pilot broadcasting and NACK/ACK broadcasting at the beginning and end of a time slot, as shown in Fig. 3, the throughput π of the system is defined as follows

$$\begin{aligned}
\pi &= \eta R_0 (1 - OP) \\
&= \left\{ e^{-\Omega_{SD}\Gamma_{th}} + \frac{1}{\lambda_2 M_2} + \left[p_2 + p_4 \left(1 - \frac{e^{-\Omega_{R2D}\Gamma_{th}}}{b_2 \lambda_2 M_2} \right) \right] \right. \\
&\quad \left. \times \frac{(1 - e^{-\Omega_{SD}\Gamma_{th}}) e^{-\Omega_{R1D}\Gamma_{th}}}{b_1 \lambda_1 M_1} \right\} \eta R_0, \quad (50)
\end{aligned}$$

Where η is the loss factor of throughput π . In addition, in order to analyze the impact of data transmission rate R_0 on system throughput π , the derivative of π with respect to R_0 is shown in Eq. (51) and Eq. (52). Furthermore, the maximum throughput π_{max} and the optimum value R_0^{max} of data transmission rate R_0 may be obtained by making the derivative $\frac{d\pi}{dR_0} = 0$.

V. NUMERICAL RESULTS

In this section, the derived analytical closed-forms and the theoretical analysis given will be numerically validated in this section. For all simulations, the system parameters are considered when the stability conditions $\psi_1 > 1$ and $\psi_2 > 1$ are satisfied. Specifically, assume S , R_1 , R_2 and D are all located in a two dimensional plane, and their position coordinates in meters are (0, 0), (30, 20), (60, -20) and (100, 0), respectively. Moreover, let the noise variance $N_0 = -50$ dBm, the path-loss parameter $\alpha = 3$, and the loss factor $\eta = 5\%$. Besides, in all the figures except Fig. 14, markers denote simulation values and lines represent the STM-based theoretical values.

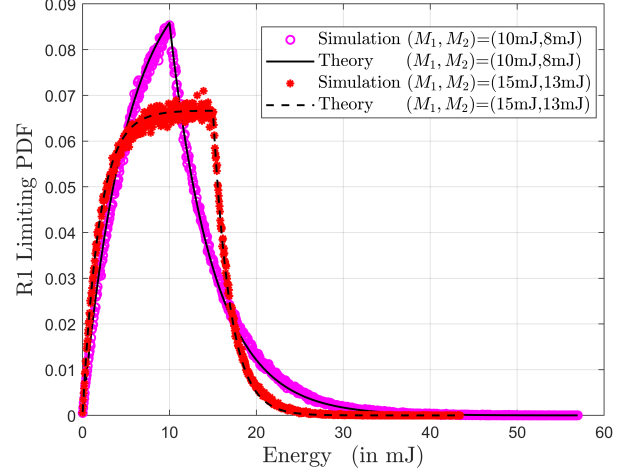


Fig. 4: Limiting PDF of energy stored in $R1$ buffer, with parameters $\frac{1}{\lambda_1} = -6$ dB, $\frac{1}{\lambda_2} = -8$ dB, $R_0 = 3$ bit/s/Hz, $P_S = 15$ dBm and two different relay energy consumptions $\{(M_1, M_2) = (10 \text{ mJ}, 8 \text{ mJ}), (15 \text{ mJ}, 13 \text{ mJ})\}$.

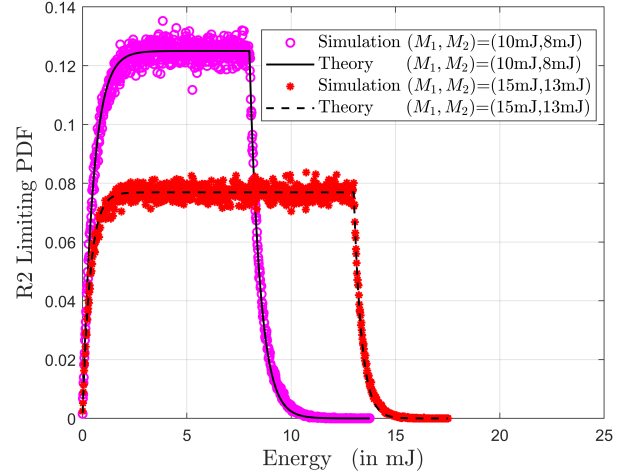


Fig. 5: Limiting PDF of energy stored in $R2$ buffer, with parameters $\frac{1}{\lambda_1} = -6$ dB, $\frac{1}{\lambda_2} = -8$ dB, $R_0 = 3$ bit/s/Hz, $P_S = 15$ dBm, and two different relay energy consumptions $\{(M_1, M_2) = (10 \text{ mJ}, 8 \text{ mJ}), (15 \text{ mJ}, 13 \text{ mJ})\}$.

Fig. 4 and Fig. 5 depict the limiting PDF of energy stored in $R1$ buffer and $R2$ buffer when the relay energy consumption is $(M_1, M_2) = (10 \text{ mJ}, 8 \text{ mJ})$ and $(M_1, M_2) = (15 \text{ mJ}, 13 \text{ mJ})$, respectively. It can be clearly seen from Fig. 4 that the theoretical PDF curve matches the simulated PDF scatters. Furthermore, the same case can be seen from Fig. 5. Both Fig. 4 and Fig. 5 effectively verifies the derived theoretical expressions in Eq. (14) and Eq. (22).

Fig. 6 and Fig. 7 present the variation of system outage probability and system throughput with relay node $R1$ energy-harvested mean $\frac{1}{\lambda_1}$ for three different data transmission rates ($R_0 = 1, 1.5$ and 2 bit/s/Hz), respectively. From Fig. 6, it can be seen that the system outage probabilities, which are obtained by simulation and theory, decrease with the increase

$$\begin{aligned}
\frac{d\pi}{dR_0} &= \frac{d\{\eta R_0 (1 - OP)\}}{dR_0} = \eta (1 - OP) - \eta R_0 \frac{dOP}{dR_0} \\
&= \left\{ e^{-\Omega_{SD}\Gamma_{th}} + \frac{1}{\lambda_2 M_2} + \left[p_2 + p_4 \left(1 - \frac{e^{-\Omega_{R2D}\Gamma_{th}}}{b_2 \lambda_2 M_2} \right) \right] \frac{(1 - e^{-\Omega_{SD}\Gamma_{th}}) e^{-\Omega_{R1D}\Gamma_{th}}}{b_1 \lambda_1 M_1} \right\} \eta + \frac{p_4 2^{R_0} \ln(2) \eta R_0 \Omega_{SD}}{b_1 b_2 \lambda_1 \lambda_2 M_1 M_2} \\
&\times e^{-(\Omega_{SD} + \Omega_{R1D} + \Omega_{R2D})\Gamma_{th}} - 2^{R_0} \ln(2) \eta R_0 \Omega_{SD} e^{-\Omega_{R1D}\Gamma_{th}} + \eta R_0 \left[p_2 + p_4 \left(1 - \frac{e^{-\Omega_{R2D}\Gamma_{th}}}{b_2 \lambda_2 M_2} \right) \right] \\
&\times \left\{ \frac{2^{R_0} \ln(2) e^{-\Omega_{R1D}\Gamma_{th}}}{b_1 \lambda_1 M_1} \left[e^{-\Omega_{R1D}\Gamma_{th}} (\Omega_{SD} + \Omega_{R1D}) - \Omega_{R1D} \right] - \frac{(1 - e^{-\Omega_{SD}\Gamma_{th}}) e^{-\Omega_{R1D}\Gamma_{th}}}{b_1^2 \lambda_1 M_1} \frac{db_1}{dR_0} \right\},
\end{aligned} \tag{51}$$

$$\begin{aligned}
\frac{db_1}{dR_0} &= p_2 2^{R_0} \ln(2) \Omega_{SD} e^{-\Omega_{SD}\Gamma_{th}} \left[e^{-\Omega_{R1D}\Gamma_{th}} + (1 - e^{-\Omega_{R1D}\Gamma_{th}}) (1 - e^{-\Omega_{SR2}\Gamma_{th}}) e^{-\Omega_{R1R2}\Gamma_{th}} \right] + p_2 (1 - e^{-\Omega_{SD}\Gamma_{th}}) \\
&\times \left\{ 2^{R_0} \ln(2) \Omega_{R1D} e^{-\Omega_{R1D}\Gamma_{th}} \left[(1 - e^{-\Omega_{SR2}\Gamma_{th}}) e^{-\Omega_{R1R2}\Gamma_{th}} - 1 \right] + 2^{R_0} \ln(2) (1 - e^{-\Omega_{R1D}\Gamma_{th}}) e^{-\Omega_{R1R2}\Gamma_{th}} \right. \\
&\times \left. \left[(\Omega_{SR2} + \Omega_{R1R2}) e^{-\Omega_{SR2}\Gamma_{th}} - \Omega_{R1R2} \right] \right\} + p_4 2^{R_0} \ln(2) e^{-\Omega_{R1D}\Gamma_{th}} \left[(\Omega_{SD} + \Omega_{R1D}) e^{-\Omega_{SD}\Gamma_{th}} - \Omega_{R1D} \right] \\
&\times \left(1 - \frac{e^{-\Omega_{R2D}\Gamma_{th}}}{b_2 \lambda_2 M_2} \right) + \frac{p_4 2^{R_0} \ln(2) \Omega_{SD} e^{-(\Omega_{SD} + \Omega_{R1D} + \Omega_{R2D})\Gamma_{th}}}{b_2 \lambda_2 M_2}.
\end{aligned} \tag{52}$$

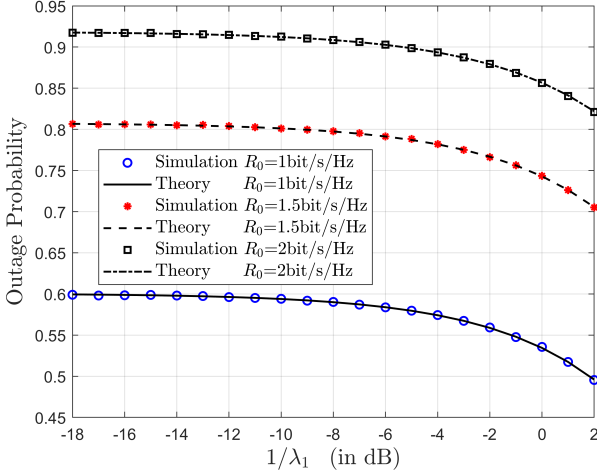


Fig. 6: Outage probability of system against relay node $R1$ energy-harvested mean $\frac{1}{\lambda_1}$, with parameters $\frac{1}{\lambda_2} = -5$ dB, $P_S = 10$ dBm, $M_1 = 15$ mJ, $M_2 = 10$ mJ and three different data transmission rates ($R_0 = 1, 1.5$ and 2 bit/s/Hz).

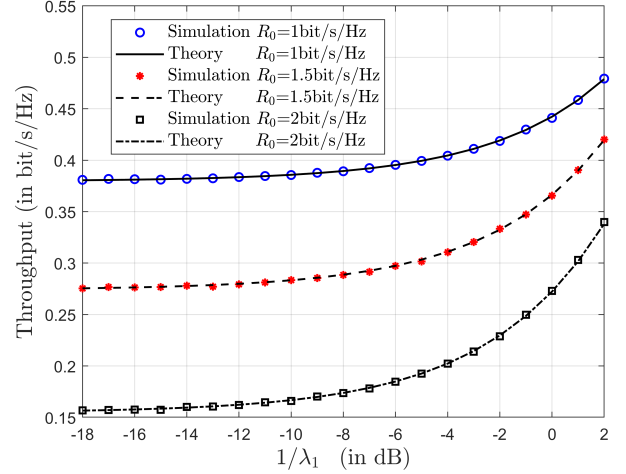


Fig. 7: Throughput of system against relay node $R1$ energy-harvested mean $\frac{1}{\lambda_1}$, with parameters $\frac{1}{\lambda_2} = -5$ dB, $P_S = 10$ dBm, $M_1 = 15$ mJ, $M_2 = 10$ mJ, and three different data transmission rates ($R_0 = 1, 1.5$ and 2 bit/s/Hz).

of $\frac{1}{\lambda_1}$ under the condition that the value of R_0 is fixed, on the contrary, decrease with the decrease of the value of R_0 when $\frac{1}{\lambda_1}$ is fixed. In contrast, in Fig. 7, the system throughputs, which are obtained by simulation and theory, increase with the increase of $\frac{1}{\lambda_1}$ under the condition that the value of R_0 is fixed, and conversely, increase with the decrease of the value of R_0 when $\frac{1}{\lambda_1}$ is fixed. This is due to the fact that the increase of $\frac{1}{\lambda_1}$ may lead to the $R1$ having more opportunities to forward the packet, and the decrease of the value of R_0 would reduce the threshold Γ_{th} which indicates D may successfully receive the packet. Moreover, from Fig. 6 and Fig. 7, it can also be seen

that the results obtained by theoretical analysis are consistent with the simulation, which effectively verifies the theoretical analysis of system outage probability and system throughput from variations of $\frac{1}{\lambda_1}$ and R_0 .

Fig. 8 and 9 illustrate the variation of system outage probability and system throughput with relay node $R2$ energy-harvested mean $\frac{1}{\lambda_2}$ for three different source transmit powers ($P_S = 10, 11$ and 12 dBm), respectively. From Fig. 8, it can be seen that the system outage probabilities, which are obtained by simulation and theory, decrease with the increase of $\frac{1}{\lambda_2}$ under the condition that the value of P_S is fixed, similarly,

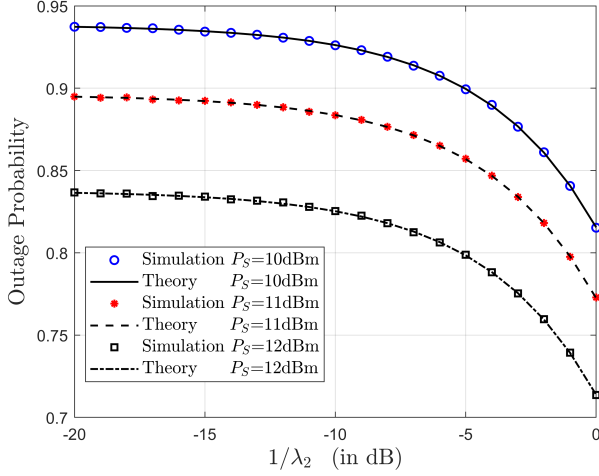


Fig. 8: Outage probability of system against relay node $R2$ energy-harvested mean $\frac{1}{\lambda_2}$, with parameters $\frac{1}{\lambda_1} = -10$ dB, $R_0 = 2$ bit/s/Hz, $M_1 = 8$ mJ, $M_2 = 8$ mJ and three different source transmit powers ($P_S = 10, 11$ and 12 dBm).

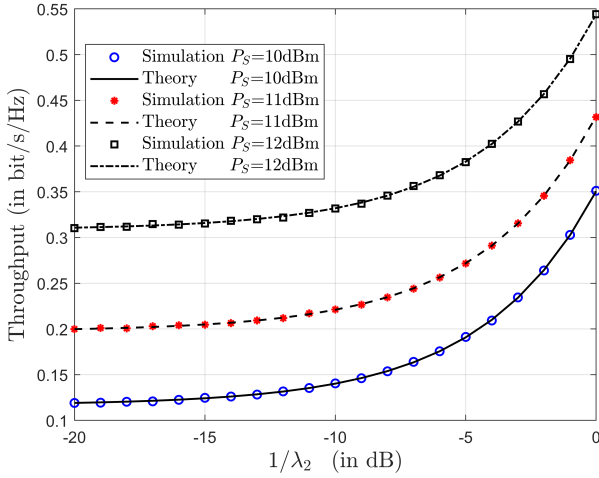


Fig. 9: Throughput of system against relay node $R2$ energy-harvested mean $\frac{1}{\lambda_2}$, with parameters $\frac{1}{\lambda_1} = -10$ dB, $R_0 = 2$ bit/s/Hz, $M_1 = 8$ mJ, $M_2 = 8$ mJ and three different source transmit powers ($P_S = 10, 11$ and 12 dBm).

decrease with the increase of the value of P_S when $\frac{1}{\lambda_2}$ is fixed. However, a comparison of Fig. 8 and Fig. 9 shows that under the same parameter setting conditions, the changing trend of system throughput in Fig. 9 is opposite to that of system outage probability in Fig. 8. This results from that the increase of $\frac{1}{\lambda_2}$ and P_S may increase the probability of $R2$ and S to forward the packet, respectively. So that the probability of D successfully receiving the packet increases. In addition, both Fig. 8 and Fig. 9 show that the results obtained by theoretical analysis are consistent with the simulation, which effectively verifies the theoretical analysis of system outage probability and system throughput by the variations of $\frac{1}{\lambda_2}$ and P_S .

Fig. 10 and Fig. 11 depict the variation of system outage probability and system throughput with the source transmit

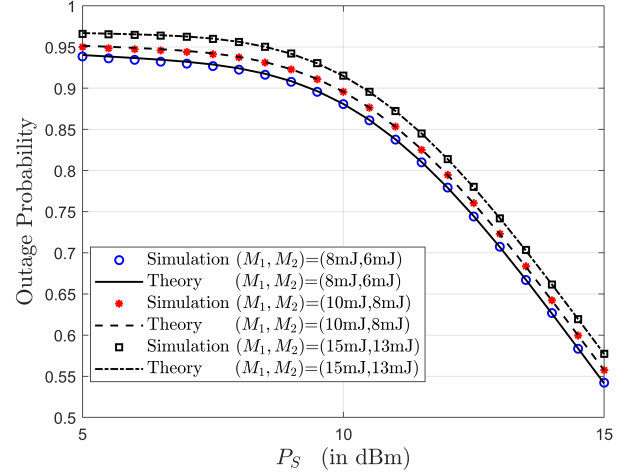


Fig. 10: Outage probability of system against source transmit power P_S , with parameters $\frac{1}{\lambda_1} = -6$ dB, $\frac{1}{\lambda_2} = -6$ dB, $R_0 = 2$ bit/s/Hz and three different relay energy consumptions $\{(M_1, M_2) = (8 \text{ mJ}, 6 \text{ mJ}), (10 \text{ mJ}, 8 \text{ mJ}) \text{ and } (15 \text{ mJ}, 13 \text{ mJ})\}$.

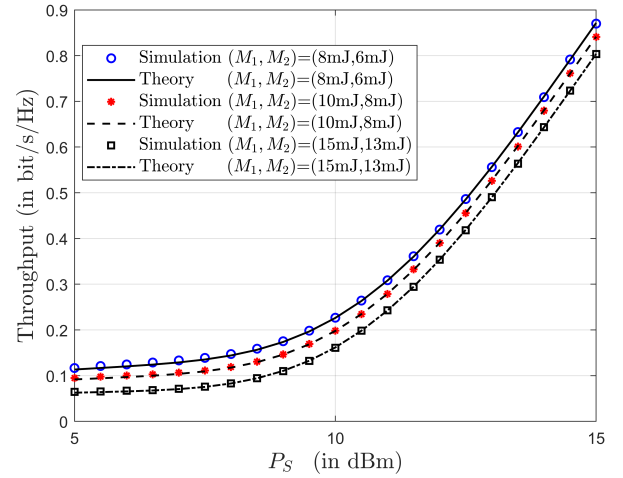


Fig. 11: Throughput of system against source transmit power P_S , with parameters $\frac{1}{\lambda_1} = -6$ dB, $\frac{1}{\lambda_2} = -6$ dB, $R_0 = 2$ bit/s/Hz and three different relay energy consumptions $\{(M_1, M_2) = (8 \text{ mJ}, 6 \text{ mJ}), (10 \text{ mJ}, 8 \text{ mJ}) \text{ and } (15 \text{ mJ}, 13 \text{ mJ})\}$.

power P_S for three different relay energy consumptions $\{(M_1, M_2) = (8 \text{ mJ}, 6 \text{ mJ}), (10 \text{ mJ}, 8 \text{ mJ}) \text{ and } (15 \text{ mJ}, 13 \text{ mJ})\}$, respectively. From Fig. 10, it can be seen that the system outage probabilities, which are obtained by simulation and theory, decrease with the increase of P_S under the condition that the value of (M_1, M_2) is fixed, on the contrary, increase with the increase of the value of (M_1, M_2) when P_S is fixed. Then, comparing Fig. 11 with Fig. 10, it is easy to find that under the same parameter setting conditions, the changing trend of system throughput in Fig. 11 is opposite to that of system outage probability in Fig. 10. Furthermore, it is also easy to find that when $P_S > 10$ dBm, compared with relay energy consumption (M_1, M_2) , the source transmits power P_S

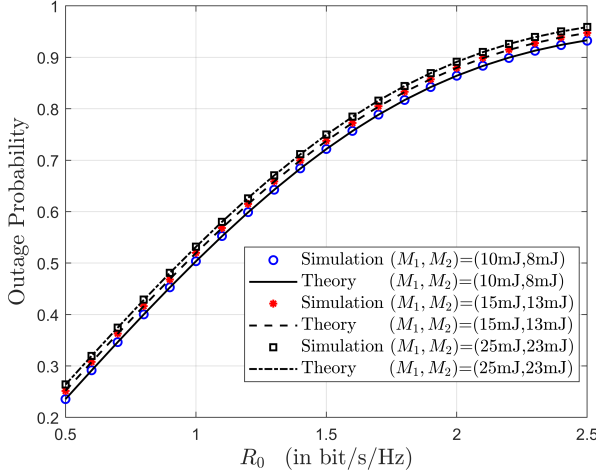


Fig. 12: Outage probability of system against data transmission rate R_0 , with parameters $\frac{1}{\lambda_1} = -7$ dB, $\frac{1}{\lambda_2} = -7$ dB, $P_S = 11$ dBm and three different relay energy consumptions $\{(M_1, M_2) = (10 \text{ mJ}, 8 \text{ mJ}), (15 \text{ mJ}, 13 \text{ mJ}) \text{ and } (25 \text{ mJ}, 23 \text{ mJ})\}$.

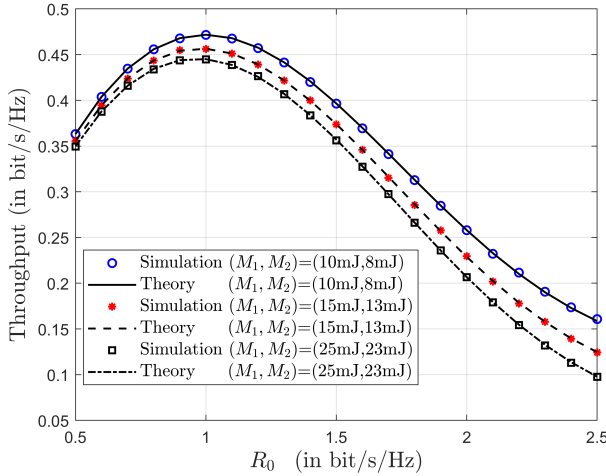


Fig. 13: Throughput of system against data transmission rate R_0 , with parameters $\frac{1}{\lambda_1} = -7$ dB, $\frac{1}{\lambda_2} = -7$ dB, $P_S = 11$ dBm and three different relay energy consumptions $\{(M_1, M_2) = (10 \text{ mJ}, 8 \text{ mJ}), (15 \text{ mJ}, 13 \text{ mJ}) \text{ and } (25 \text{ mJ}, 23 \text{ mJ})\}$.

has a greater impact on system outage probability and system throughput. This is because with the gradual increase of source transmission power P_S , the probability of the packet directly transmitted from the source node S to the destination node D increases significantly. Meanwhile, it can be seen from both Fig. 10 and Fig. 11 that the theoretical results fit into the simulation results, which effectively verifies the theoretical analysis of system outage probability and system throughput from the variations of P_S and (M_1, M_2) .

Fig. 12 and Fig. 13 present the variation of system outage probability and system throughput with the data transmission rate R_0 for three different relay energy consumptions

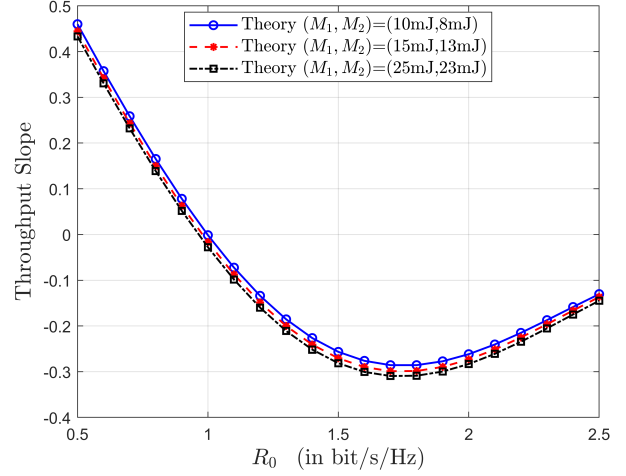


Fig. 14: Slope of system theoretical throughput against data transmission rate R_0 , with parameters $\frac{1}{\lambda_1} = -7$ dB, $\frac{1}{\lambda_2} = -7$ dB, $P_S = 11$ dBm and three different relay energy consumptions $\{(M_1, M_2) = (10 \text{ mJ}, 8 \text{ mJ}), (15 \text{ mJ}, 13 \text{ mJ}) \text{ and } (25 \text{ mJ}, 23 \text{ mJ})\}$.

$\{(M_1, M_2) = (10 \text{ mJ}, 8 \text{ mJ}), (15 \text{ mJ}, 13 \text{ mJ}) \text{ and } (25 \text{ mJ}, 23 \text{ mJ})\}$, respectively. From Fig. 12, it can be seen that the system outage probabilities, which are obtained by simulation and theory, increase with the increase of R_0 or (M_1, M_2) . Especially compared with relay energy consumption (M_1, M_2) , data transmission rate R_0 has a greater impact on system outage probabilities. This is due to the increase of the value of R_0 would significantly increase the threshold Γ_{th} , which may greatly reduce the probability of node D successfully receiving the packet. However, from Fig. 13, it can be seen that for three different relay energy consumptions $\{(M_1, M_2) = (10 \text{ mJ}, 8 \text{ mJ}), (15 \text{ mJ}, 13 \text{ mJ}) \text{ and } (25 \text{ mJ}, 23 \text{ mJ})\}$, the system throughputs, which are obtained by simulation and theory, increase with the increase of R_0 when $R_0 < 1$ bit/s/Hz, and conversely, decrease with the increase of R_0 when the $R_0 > 1$ bit/s/Hz. Therefore, it can be concluded that under this system parameter setting, the optimal throughput can be obtained when R_0 is about 1 bit/s/Hz. Moreover, both Fig. 12 and Fig. 13 show that the curves obtained from the theoretical analysis are consistent with the simulation values, which effectively verifies the theoretical analysis of system outage probability and system throughput from variations of R_0 and (M_1, M_2) .

Fig. 14 illustrates the variation of slope of theoretical throughput curves to data transmission rate R_0 for three different relay energy consumptions $\{(M_1, M_2) = (10 \text{ mJ}, 8 \text{ mJ}), (15 \text{ mJ}, 13 \text{ mJ}) \text{ and } (25 \text{ mJ}, 23 \text{ mJ})\}$, respectively. From Fig. 14, it can be clearly observed that $R_0 = 1$ bit/s/Hz is approximately the point where the slopes of the three different theoretical throughput curves are zero. Moreover, the slopes corresponding to points on the left of $R_0 = 1$ bit/s/Hz are positive, while the slopes corresponding to points on the right of $R_0 = 1$ bit/s/Hz is negative. That is, when R_0 is about 1 bit/s/Hz, the optimal throughput can be obtained,

which is consistent with the analysis result in Fig. 13, and also effectively verifies the theoretical analysis of the system throughput.

VI. CONCLUSION

This paper proposes the OR aided cooperative communication network with EH. Where the OR protocol is proposed to select the packet transmission path based on the node transmission priority. Additionally, the STM-based algorithm is proposed to find the probability distribution of the CBN set. Using both DCSMC model and the probability distribution, the existence conditions and analytical expressions of the limiting distribution of energy in energy buffers are determined. Then, based on the limiting distribution of energy in energy buffers, the network outage probability and throughput are analyzed, and the corresponding closed-form expressions are given. Furthermore, various simulation findings show that the simulation results are in line with the theoretical analysis results. The relay system containing more than two EH relay nodes is proposed as a future research direction.

APPENDIX A PROOF OF THEOREM 1

According to the energy storage process $B_2(i)$ with the infinite-size energy buffer in Eq. (10), the variable $O_R(i)$ is defined by [17, Appendix B]

$$O_R(i) = \begin{cases} 1, & \mathbb{P}_{22} \\ 0, & \mathbb{P}_{21} \end{cases} \quad (53)$$

where \mathbb{P}_{21} and \mathbb{P}_{22} have been given in Eq. (11) and Eq. (12), respectively. Implying Eq. (53), the energy storage process in Eq. (10) can be re-expressed as follows

$$B_2(i+1) - B_2(i) = X_2(i) - M_2 O_R(i). \quad (54)$$

According to the law of large numbers, the average energy harvesting rate can be obtained as follows

$$\mathbb{E}[X_2(i)] = \lim_{N \rightarrow \infty} \frac{1}{N} \sum_{i=1}^N X_2(i), \quad (55)$$

similarly, the average energy consumption rate can be given by

$$\begin{aligned} \mathbb{E}[M_2 O_R(i)] &= \lim_{N \rightarrow \infty} \frac{1}{N} \sum_{i=1}^N M_2 O_R(i) \\ &\leq M_2 \left\{ \lim_{N \rightarrow \infty} \frac{1}{N} \sum_{i=1}^N O_R(i) \right\}. \end{aligned} \quad (56)$$

moreover,

$$\begin{aligned} \mathbb{E}[O_R(i)] &= \lim_{N \rightarrow \infty} \frac{1}{N} \sum_{i=1}^N O_R(i) \\ &= 1 \times \Pr\{O_R(i) = 1\} + 0 \times \Pr\{O_R(i) = 0\} \\ &= \Pr\{\mathbf{S}(i) = \mathbf{s}_3, C_9(i)\} + \Pr\{\mathbf{S}(i) = \mathbf{s}_4, C_9(i)\} \\ &\leq (p_3 + p_4) (1 - e^{-\Omega_{SD}\Gamma_{th}}) e^{-\Omega_{RD}\Gamma_{th}}. \end{aligned} \quad (57)$$

From Eq. (56) and Eq. (57), we obtain

$$\mathbb{E}[M_2 O_R(i)] \leq M_2 (p_3 + p_4) (1 - e^{-\Omega_{SD}\Gamma_{th}}) e^{-\Omega_{RD}\Gamma_{th}}. \quad (58)$$

If $\psi_1 \leq 1$, from Eq. (13), we get

$$\mathbb{E}[X_2(i)] \geq M_2 (p_3 + p_4) (1 - e^{-\Omega_{SD}\Gamma_{th}}) e^{-\Omega_{RD}\Gamma_{th}}. \quad (59)$$

Therefore, if $\psi_1 \leq 1$, from Eq. (55), Eq. (56), Eq. (58) and Eq. (59), we obtain

$$\lim_{N \rightarrow \infty} \frac{1}{N} \sum_{i=1}^N X_2(i) \geq \lim_{N \rightarrow \infty} \frac{1}{N} \sum_{i=1}^N M_2 O_R(i). \quad (60)$$

According to Eq. (54) and Eq. (60), we have

$$\lim_{N \rightarrow \infty} \frac{1}{N} \sum_{i=1}^N B_2(i+1) \geq \lim_{N \rightarrow \infty} \frac{1}{N} \sum_{i=1}^N B_2(i). \quad (61)$$

Clearly, if the inequality condition holds in Eq. (61), the comparison of between $B_2(i+1)$ and $B_2(i)$ shows that the energy accumulates in the buffer over time slot, i.e., $\lim_{i \rightarrow \infty} \mathbb{E}[B_2(i)] = \infty$. Therefore, the stationary distribution of $B_2(i)$ does not exist, and after a finite number of time slots, $B_2(i) > M_2$ almost always hold [7, Appendix A]. In addition, if the equality condition holds in Eq. (60), according to Eq. (60) and Eq. (56), we get

$$\lim_{N \rightarrow \infty} \frac{1}{N} \sum_{i=1}^N X_2(i) = \lim_{N \rightarrow \infty} \frac{1}{N} \sum_{i=1}^N M_2 O_R(i). \quad (62)$$

Eq. (62) indicates that in the energy buffer with the DCSMC model, the average energy harvesting rate equals the average energy consumption rate, which is unstable [33]. Therefore, the buffer may almost always provide M_2 amount of energy.

APPENDIX B PROOF OF THEOREM 2

According to the total probability theorem, \mathbb{P}_{21} and \mathbb{P}_{22} together constitutes a complete set of events accompanying event $B_2(i+1)$. Therefore, the cumulative distribution function (CDF) of $B_2(i+1)$ in storage process in Eq. (10) may be evaluated as follows [17, Appendix C]

$$\begin{aligned} \Pr\{B_2(i+1) \leq x\} &= \Pr\{B_2(i) + X_2(i) \leq x, \mathbf{S}(i) = \mathbf{s}_1\} \\ &+ \Pr\{B_2(i) + X_2(i) \leq x, \mathbf{S}(i) = \mathbf{s}_2\} \\ &+ \Pr\{B_2(i) + X_2(i) \leq x, \mathbf{S}(i) = \mathbf{s}_3, C_1(i)\} \\ &+ \Pr\{B_2(i) + X_2(i) \leq x, \mathbf{S}(i) = \mathbf{s}_3, \overline{C_1}(i), B_2(i) < M_2\} \\ &+ \Pr\{B_2(i) + X_2(i) \leq x, \mathbf{S}(i) = \mathbf{s}_3, \overline{C_1}(i), B_2(i) \geq M_2, \\ &\quad \gamma_{RD}(i) < \Gamma_{th}\} \\ &+ \Pr\{B_2(i) + X_2(i) \leq x, \mathbf{S}(i) = \mathbf{s}_4, C_1(i)\} \\ &+ \Pr\{B_2(i) + X_2(i) \leq x, \mathbf{S}(i) = \mathbf{s}_4, \overline{C_1}(i), B_2(i) < M_2\} \\ &+ \Pr\{B_2(i) + X_2(i) \leq x, \mathbf{S}(i) = \mathbf{s}_4, \overline{C_1}(i), B_2(i) \geq M_2, \\ &\quad \gamma_{RD}(i) < \Gamma_{th}\} \\ &+ \Pr\{B_2(i) + X_2(i) - M_2 \leq x, \mathbf{S}(i) = \mathbf{s}_3, C_9(i)\} \\ &+ \Pr\{B_2(i) + X_2(i) - M_2 \leq x, \mathbf{S}(i) = \mathbf{s}_4, C_9(i)\}. \end{aligned} \quad (63)$$

Let $B_2(i) = \mu_2$, $X_2(i) = X_2$, $\mathbf{S}(i) = \mathbf{S}$, $C_1(i) = C_1$, $\overline{C_1}(i) = \overline{C_1}$, $C_9(i) = C_9$, and $\gamma_{R2D}(i) = \gamma_{R2D}$. Eq. (63) may be presented by

$$\begin{aligned} & \Pr\{B_2(i+1) \leq x\} \\ &= \Pr\{\mu_2 + X_2 \leq x, \mathbf{S} = \mathbf{s}_1\} \\ &+ \Pr\{\mu_2 + X_2 \leq x, \mathbf{S} = \mathbf{s}_2\} \\ &+ \Pr\{\mu_2 + X_2 \leq x, \mathbf{S} = \mathbf{s}_3, C_1\} \\ &+ \Pr\{\mu_2 + X_2 \leq x, \mathbf{S} = \mathbf{s}_3, \overline{C_1}, B_2(i) < M_2\} \\ &+ \Pr\{\mu_2 + X_2 \leq x, \mathbf{S} = \mathbf{s}_3, \overline{C_1}, B_2 \geq M_2, \gamma_{R2D} < \Gamma_{th}\} \\ &+ \Pr\{\mu_2 + X_2 \leq x, \mathbf{S} = \mathbf{s}_4, C_1\} \\ &+ \Pr\{\mu_2 + X_2 \leq x, \mathbf{S} = \mathbf{s}_4, \overline{C_1}, \mu_2 < M_2\} \\ &+ \Pr\{\mu_2 + X_2 \leq x, \mathbf{S} = \mathbf{s}_4, \overline{C_1}, \mu_2 \geq M_2, \gamma_{R2D} < \Gamma_{th}\} \\ &+ \Pr\{\mu_2 + X_2 - M_2 \leq x, \mathbf{S} = \mathbf{s}_3, C_9\} \\ &+ \Pr\{\mu_2 + X_2 - M_2 \leq x, \mathbf{S} = \mathbf{s}_4, C_9\}. \end{aligned} \quad (64)$$

Denote $G_2^{i+1}(x)$ as the CDF of $B_2(i+1)$, namely, $\Pr\{B_2(i+1) \leq x\} = G_2^{i+1}(x)$. When $i \rightarrow \infty$, if the buffer reaches its steady state, it follows that, $\Pr\{B_2(i+1) \leq x\} = G_2^{i+1}(x) = G_2^i(x) = G_2(x)$. In this state, Eq. (64) may be written as follows

$$\begin{aligned} G_2(x) &= (p_1 + p_2) \int_{\mu_2=0}^x F_{X_2}(x - \mu_2) g_2(\mu_2) d\mu_2 \\ &+ (p_3 + p_4) \int_{r_1=\Gamma_{th}}^{\infty} \int_{\mu_2=0}^x F_{X_2}(x - \mu_2) g_2(\mu_2) \\ &\times f_{\gamma_{SD}}(r_1) d\mu_2 dr_1 \\ &+ (p_3 + p_4) \int_{r_1=0}^{\Gamma_{th}} \int_{\mu_2=0}^{\min(x, M_2)} F_{X_2}(x - \mu_2) g_2(\mu_2) \\ &\times f_{\gamma_{SD}}(r_1) d\mu_2 dr_1 \\ &+ (p_3 + p_4) \int_{r_1=0}^{\Gamma_{th}} \int_{r_2=0}^{\Gamma_{th}} \int_{\mu_2=M_2}^x F_{X_2}(x - \mu_2) g_2(\mu_2) \\ &\times f_{\gamma_{SD}}(r_1) f_{\gamma_{R2D}}(r_2) d\mu_2 dr_1 dr_2 \\ &+ (p_3 + p_4) \int_{r_1=0}^{\Gamma_{th}} \int_{r_2=\Gamma_{th}}^{\infty} \int_{\mu_2=M_2}^{x+M_2} F_{X_2}(x + M_2 - \mu_2) \\ &\times g_2(\mu_2) f_{\gamma_{SD}}(r_1) f_{\gamma_{R2D}}(r_2) d\mu_2 dr_1 dr_2, \end{aligned} \quad (65)$$

where $F_{X_2}(x) = 1 - e^{-\lambda_2 x}$ is the CDF of X_2 . $g_2(x)$ is the derivative of $G_2(x)$. In addition, $f_{\gamma_{SD}}(r_1) = \Omega_{SD} e^{-\Omega_{SD} r_1}$ and $f_{\gamma_{R2D}}(r_2) = \Omega_{R2D} e^{-\Omega_{R2D} r_2}$ are the PDFs of γ_{SD} and γ_{R2D} , respectively. Substituting $f_{\gamma_{SD}}(r_1)$ and $f_{\gamma_{R2D}}(r_2)$ in Eq. (65), and simplifying Eq. (65), we arrive at

$$G_2(x) = \begin{cases} G_{21}(x), & 0 \leq x < M_2 \\ G_{22}(x), & x \geq M_2 \end{cases} \quad (66)$$

where,

$$\begin{aligned} G_{21}(x) &= \int_{\mu_2=0}^x F_{X_2}(x - \mu_2) g_2(\mu_2) d\mu_2 \\ &+ (p_3 + p_4) (1 - e^{-\Omega_{SD} \Gamma_{th}}) e^{-\Omega_{R2D} \Gamma_{th}} \\ &\times \int_{\mu_2=M_2}^{x+M_2} F_{X_2}(x + M_2 - \mu_2) g_2(\mu_2) d\mu_2, \end{aligned} \quad (67)$$

$$\begin{aligned} G_{22}(x) &= \int_{\mu_2=0}^{M_2} F_{X_2}(x - \mu_2) g_2(\mu_2) d\mu_2 \\ &+ [1 - (p_3 + p_4) (1 - e^{-\Omega_{SD} \Gamma_{th}}) e^{-\Omega_{R2D} \Gamma_{th}}] \\ &\times \int_{\mu_2=M_2}^x F_{X_2}(x - \mu_2) g_2(\mu_2) d\mu_2 \\ &+ [(p_3 + p_4) (1 - e^{-\Omega_{SD} \Gamma_{th}}) e^{-\Omega_{R2D} \Gamma_{th}}] \\ &\times \int_{\mu_2=M_2}^{x+M_2} F_{X_2}(x + M_2 - \mu_2) g_2(\mu_2) d\mu_2. \end{aligned} \quad (68)$$

According to Eq. (66), the PDF $g_2(x)$ may be defined as

$$g_2(x) = \begin{cases} g_{21}(x), & 0 \leq x < M_2 \\ g_{22}(x), & x \geq M_2. \end{cases} \quad (69)$$

After substituting Eq. (69) into Eq. (68), the derivatives about x on both sides of Eq. (68) may be obtained

$$\begin{aligned} g_{22}(x) &= \int_{\mu_2=0}^{M_2} f_{X_2}(x - \mu_2) g_{21}(\mu_2) d\mu_2 \\ &+ a_2 \int_{\mu_2=M_2}^x f_{X_2}(x - \mu_2) g_{22}(\mu_2) d\mu_2 \\ &+ b_2 \int_{\mu_2=M_2}^{x+M_2} f_{X_2}(x + M_2 - \mu_2) g_{22}(\mu_2) d\mu_2, \end{aligned} \quad (70)$$

where,

$$a_2 = [1 - (p_3 + p_4) (1 - e^{-\Omega_{SD} \Gamma_{th}}) e^{-\Omega_{R2D} \Gamma_{th}}], \quad (71)$$

$$b_2 = [(p_3 + p_4) (1 - e^{-\Omega_{SD} \Gamma_{th}}) e^{-\Omega_{R2D} \Gamma_{th}}]. \quad (72)$$

Clearly, $a_2 + b_2 = 1$. Furthermore, there is evidence that storage process in Eq. (10) possesses a unique stationary distribution [7, Appendix B], when $M_2 > \mathbb{E}[X_2(i)] = 1/\lambda_2$. In other words, $g_2(x)$ has unique solution. Furthermore, $g_{22}(x)$ be assumed to have an exponential-type solution expressed by $g_{22}(x) = k_2 e^{Q_2 x}$ [7, Appendix C]. Substituting $g_{22}(x) = k_2 e^{Q_2 x}$ and $f_{X_2}(x) = \lambda_2 e^{-\lambda_2 x}$ into Eq. (70), we obtain

$$\begin{aligned} k_2 e^{Q_2 x} &= \int_{\mu_2=0}^{M_2} \lambda_2 e^{-\lambda_2 (x - \mu_2)} g_{21}(\mu_2) d\mu_2 \\ &+ a_2 \int_{\mu_2=M_2}^x \lambda_2 e^{-\lambda_2 (x - \mu_2)} k_2 e^{Q_2 \mu_2} d\mu_2 \\ &+ b_2 \int_{\mu_2=M_2}^{x+M_2} \lambda_2 e^{-\lambda_2 (x + M_2 - \mu_2)} k_2 e^{Q_2 \mu_2} d\mu_2. \end{aligned} \quad (73)$$

Simplifying Eq. (73), we have

$$\begin{aligned} k_2 e^{Q_2 x} &= \lambda_2 e^{-\lambda_2 x} \int_{\mu_2=0}^{M_2} e^{\lambda_2 \mu_2} g_{21}(\mu_2) d\mu_2 \\ &- \frac{\lambda_2 k_2 [b_2 + a_2 e^{\lambda_2 M_2}]}{\lambda_2 + Q_2} e^{(Q_2 M_2 - \lambda_2 x)} \\ &+ \frac{b_2 \lambda_2 e^{Q_2 M_2} + a_2 \lambda_2}{\lambda_2 + Q_2} k_2 e^{Q_2 x}. \end{aligned} \quad (74)$$

For the correctness of postulating $g_{22}(x) = k_2 e^{Q_2 x}$, both sides of Eq. (74) must be equal. Hence, we get

$$\begin{cases} \frac{b_2 \lambda_2 e^{Q_2 M_2} + a_2 \lambda_2}{\lambda_2 + Q_2} = 1, \end{cases} \quad (75a)$$

$$\begin{cases} \frac{k_2 e^{Q_2 M_2} [b_2 + a_2 e^{\lambda_2 M_2}]}{\lambda_2 + Q_2} = \int_{\mu_2=0}^{M_2} e^{\lambda_2 \mu_2} g_{21}(\mu_2) d\mu_2. \end{cases} \quad (75b)$$

It can be seen from Eq. (75a) that $Q_{20} = 0$ is one of the solutions of Q_2 in Eq. (75a), but this solution does not meet the condition that $g_{22}(x)$ is a finite distribution. Additionally, the other solution Q_{21} of Q_2 in Eq. (75a) can be obtained by simplifying Eq. (75a) as

$$b_2 \lambda_2 e^{Q_2 M_2} = \lambda_2 - a_2 \lambda_2 + Q_2 = b_2 \lambda_2 + Q_2. \quad (76)$$

Using Lambert W function, the solution Q_{21} of Q_2 can be obtained as follows

$$Q_{21} = \frac{-W(-b_2 \lambda_2 M_2 e^{-b_2 \lambda_2 M_2})}{M_2} - b_2 \lambda_2. \quad (77)$$

According to the property of Lambert W function, when $b_2 \lambda_2 M_2 \leq 1$, $W(-b_2 \lambda_2 M_2 e^{-b_2 \lambda_2 M_2}) = -b_2 \lambda_2 M_2$ so that $Q_{21} = Q_{20} = 0$. On the contrary, when $b_2 \lambda_2 M_2 > 1$, $W(-b_2 \lambda_2 M_2 e^{-b_2 \lambda_2 M_2}) > -b_2 \lambda_2 M_2$ so that $Q_{21} < 0$, ensuring the finite distribution of $g_{22}(x)$. Thus, for the stationary distribution of $g_{22}(x)$, we obtain

$$Q_2 = \frac{-W(-b_2 \lambda_2 M_2 e^{-b_2 \lambda_2 M_2})}{M_2} - b_2 \lambda_2, \quad b_2 \lambda_2 M_2 > 1. \quad (78)$$

Similarly, when $0 \leq x < M_2$, substituting Eq. (69) into Eq. (67), the derivatives about x on both sides of Eq. (67) can be obtained

$$g_{21}(x) = b_2 \int_{\mu_2=M_2}^{x+M_2} f_{X_2}(x+M_2-\mu_2) g_{22}(\mu_2) d\mu_2 + \int_{\mu_2=0}^x f_{X_2}(x-\mu_2) g_{21}(\mu_2) d\mu_2. \quad (79)$$

Substituting $g_{22}(x) = k_2 e^{Q_2 x}$ and $f_{X_2}(x) = \lambda_2 e^{-\lambda_2 x}$ into Eq. (79), we get

$$g_{21}(x) = \lambda_2 \int_{\mu_2=0}^x e^{-\lambda_2(x-\mu_2)} g_{21}(\mu_2) d\mu_2 + \frac{b_2 k_2 \lambda_2 e^{Q_2 M_2}}{\lambda_2 + Q_2} (e^{Q_2 x} - e^{-\lambda_2 x}). \quad (80)$$

Let $r_2(x) = \frac{b_2 k_2 \lambda_2 e^{Q_2 M_2}}{\lambda_2 + Q_2} (e^{Q_2 x} - e^{-\lambda_2 x})$, and the integral equation in Eq. (80) can be rewritten as follows

$$g_{21}(x) = \lambda_2 \int_{\mu_2=0}^x e^{-\lambda_2(x-\mu_2)} g_{21}(\mu_2) d\mu_2 + r_2(x). \quad (81)$$

Clearly, Eq. (81) is a Volterra integral equation of the second kind, whose solution is given by [6], [17] and [34, eq. 2.2.1]

$$g_{21}(x) = r_2(x) + \lambda_2 \int_{t=0}^x r_2(t) dt. \quad (82)$$

Substituting $r_2(x)$ into Eq. (82), we obtain

$$g_{21}(x) = \frac{b_2 k_2 \lambda_2 e^{Q_2 M_2}}{\lambda_2 + Q_2} (e^{Q_2 x} - e^{-\lambda_2 x}) + \lambda_2 \int_{t=0}^x \frac{b_2 k_2 \lambda_2 e^{Q_2 M_2}}{\lambda_2 + Q_2} (e^{Q_2 t} - e^{-\lambda_2 t}) dt = \frac{b_2 k_2 \lambda_2 e^{Q_2 M_2}}{Q_2} (e^{Q_2 x} - 1). \quad (83)$$

According to the unit area condition on $g_2(x)$, we have

$$\int_{x=0}^{\infty} g_2(x) dx = \int_{x=0}^{M_2} g_{21}(x) dx + \int_{x=M_2}^{\infty} g_{22}(x) dx = 1. \quad (84)$$

Substituting $g_{21}(x) = \frac{b_2 k_2 \lambda_2 e^{Q_2 M_2} (e^{Q_2 x} - 1)}{Q_2}$ and $g_{22}(x) = k_2 e^{Q_2 x}$ into Eq. (84), we get

$$\frac{b_2 k_2 \lambda_2 e^{Q_2 M_2}}{Q_2} \int_{x=0}^{M_2} (e^{Q_2 x} - 1) dx + k_2 \int_{x=M_2}^{\infty} e^{Q_2 x} dx = 1. \quad (85)$$

Simplifying Eq. (85), we have

$$\frac{b_2 k_2 \lambda_2 e^{Q_2 M_2}}{Q_2} \left[\frac{e^{Q_2 M_2} - 1}{Q_2} - M_2 \right] - \frac{k_2 e^{Q_2 M_2}}{Q_2} = 1. \quad (86)$$

Substituting Eq. (76) into Eq. (86), then simplifying Eq. (86), the value of k_2 can be obtained as follows

$$k_2 = \frac{-Q_2}{M_2 (b_2 \lambda_2 + Q_2)}. \quad (87)$$

Substituting Eq. (76) and Eq. (87) into Eq. (83), we arrive at

$$g_{21}(x) = \frac{1 - e^{Q_2 x}}{M_2}. \quad (88)$$

Substituting Eq. (88) into the right side of Eq. (75b), we obtain

$$\int_{\mu_2=0}^{M_2} e^{\lambda_2 \mu_2} g_{21}(\mu_2) d\mu_2 = \int_{\mu_2=0}^{M_2} \frac{(1 - e^{Q_2 \mu_2}) e^{\lambda_2 \mu_2}}{M_2} d\mu_2 = \frac{1 - e^{(\lambda_2 + Q_2) M_2}}{(\lambda_2 + Q_2) M_2} - \frac{1 - e^{\lambda_2 M_2}}{\lambda_2 M_2}. \quad (89)$$

The equation in Eq. (76) leads us to conclude $\lambda_2 M_2 = \frac{(\lambda_2 + Q_2) M_2}{b_2 e^{Q_2 M_2} + a_2}$. Substituting this conclusion in Eq. (89), we have

$$\int_{\mu_2=0}^{M_2} e^{\lambda_2 \mu_2} g_{21}(\mu_2) d\mu_2 = \frac{(1 - e^{Q_2 M_2}) (b_2 + a_2 e^{\lambda_2 M_2})}{(\lambda_2 + Q_2) M_2}. \quad (90)$$

Similarly, the conclude $1 - e^{Q_2 M_2} = \frac{-Q_2}{b_2 \lambda_2}$ may be obtained from Eq. (76). Substituting this conclusion in Eq. (90), we arrive at

$$\begin{aligned} \int_{\mu_2=0}^{M_2} e^{\lambda_2 \mu_2} g_{21}(\mu_2) d\mu_2 &= \frac{-Q_2 (b_2 + a_2 e^{\lambda_2 M_2})}{(\lambda_2 + Q_2) M_2 b_2 \lambda_2} \\ &= \frac{-Q_2 e^{Q_2 M_2} (b_2 + a_2 e^{\lambda_2 M_2})}{(\lambda_2 + Q_2) M_2 b_2 \lambda_2 e^{Q_2 M_2}} \\ &= \frac{-Q_2 e^{Q_2 M_2} (b_2 + a_2 e^{\lambda_2 M_2})}{M_2 (b_2 \lambda_2 + Q_2) (\lambda_2 + Q_2)} \\ &= \frac{k_2 e^{Q_2 M_2} (b_2 + a_2 e^{\lambda_2 M_2})}{\lambda_2 + Q_2}. \end{aligned} \quad (91)$$

Now, it can be shown that $g_{21}(x)$ satisfies the condition in Eq. (75b). Therefore, there is no doubt that the unique solution $g_{21}(x)$ in Eq. (88) for Eq. (79) and the unique solution $g_{22}(x) = k_2 e^{Q_2 x}$ for Eq. (70) are obtained.

APPENDIX C
PROOF OF THEOREM 3

According to the total probability theorem, \mathbb{P}_{11} and \mathbb{P}_{12} , the CDF of $B_1(i+1)$ in storage process in Eq. (18) may be evaluated as follows

$$\begin{aligned} \Pr\{B_1(i+1) \leq x\} &= \Pr\{B_1(i) + X_1(i) \leq x, \mathbf{S}(i) = \mathbf{s}_1\} \\ &+ \Pr\{B_1(i) + X_1(i) \leq x, \mathbf{S}(i) = \mathbf{s}_3\} \\ &+ \Pr\{\Theta_1\} + \Pr\{\Theta_2\} \\ &+ \Pr\{B_1(i) + X_1(i) - M_1 \leq x, \mathbf{S}(i) = \mathbf{s}_2, C_5(i)\} \\ &+ \Pr\{B_1(i) + X_1(i) - M_1 \leq x, \mathbf{S}(i) = \mathbf{s}_2, C_8(i)\} \\ &+ \Pr\{B_1(i) + X_1(i) - M_1 \leq x, \mathbf{S}(i) = \mathbf{s}_4, C_{10}(i)\} \\ &+ \Pr\{B_1(i) + X_1(i) - M_1 \leq x, \mathbf{S}(i) = \mathbf{s}_4, C_{11}(i)\}, \end{aligned} \quad (92)$$

where, $\Pr\{\Theta_1\}$ is presented as follows

$$\begin{aligned} \Pr\{\Theta_1\} &= \Pr\{B_1(i) + X_1(i) \leq x, \mathbf{S}(i) = \mathbf{s}_2, C_1(i)\} \\ &+ \Pr\{B_1(i) + X_1(i) \leq x, \mathbf{S}(i) = \mathbf{s}_2, \overline{C_1}(i), B_1(i) < M_1\} \\ &+ \Pr\{B_1(i) + X_1(i) \leq x, \mathbf{S}(i) = \mathbf{s}_2, \overline{C_1}(i), B_1(i) \geq M_1, \\ &\gamma_{R1D}(i) < \Gamma_{th}, \gamma_{SR2}(i) \geq \Gamma_{th}\} \\ &+ \Pr\{B_1(i) + X_1(i) \leq x, \mathbf{S}(i) = \mathbf{s}_2, \overline{C_1}(i), B_1(i) \geq M_1, \\ &\gamma_{R1D}(i) < \Gamma_{th}, \gamma_{SR2}(i) \geq \Gamma_{th}, \gamma_{R1R2}(i) < \Gamma_{th}\}, \end{aligned} \quad (93)$$

and $\Pr\{\Theta_2\}$ is given by

$$\begin{aligned} \Pr\{\Theta_2\} &= \Pr\{B_1(i) + X_1(i) \leq x, \mathbf{S}(i) = \mathbf{s}_4, C_1(i)\} \\ &+ \Pr\{B_1(i) + X_1(i) \leq x, \mathbf{S}(i) = \mathbf{s}_4, C_9(i)\} \\ &+ \Pr\{B_1(i) + X_1(i) \leq x, \mathbf{S}(i) = \mathbf{s}_4, \overline{C_1}(i), B_2(i) \geq M_2, \\ &\gamma_{R2D}(i) < \Gamma_{th}, B_1(i) \geq M_1, \gamma_{R1D}(i) < \Gamma_{th}\} \\ &+ \Pr\{B_1(i) + X_1(i) \leq x, \mathbf{S}(i) = \mathbf{s}_4, \overline{C_1}(i), B_2(i) \geq M_2, \\ &\gamma_{R2D}(i) < \Gamma_{th}, B_1(i) < M_1\} \\ &+ \Pr\{B_1(i) + X_1(i) \leq x, \mathbf{S}(i) = \mathbf{s}_4, \overline{C_1}(i), B_2(i) < M_2, \\ &B_1(i) \geq M_1, \gamma_{R1D}(i) < \Gamma_{th}\} \\ &+ \Pr\{B_1(i) + X_1(i) \leq x, \mathbf{S}(i) = \mathbf{s}_4, \overline{C_1}(i), B_2(i) < M_2, \\ &B_1(i) < M_1\}. \end{aligned} \quad (94)$$

Since γ_{SD} , γ_{SR2} , γ_{R1D} , γ_{R1R2} and γ_{R2D} obey the exponential distribution with parameters Ω_{SD} , Ω_{SR2} , Ω_{R1D} , Ω_{R1R2} and Ω_{R2D} , respectively. In addition, the probabilities of $\Pr\{B_2(i) \geq M_R\}$ has been given in Eq. (16). When $i \rightarrow \infty$, Eq. (92) is written as follows

$$\begin{aligned} G_1(x) &= a_{11} \int_{\mu_1=0}^x F_{X_1}(x - \mu_1) g_1(\mu_1) d\mu_1 \\ &+ a_{12} \int_{\mu_1=0}^{\min(x, M_1)} F_{X_1}(x - \mu_1) g_1(\mu_1) d\mu_1 \\ &+ a_{13} \int_{\mu_1=M_1}^x F_{X_1}(x - \mu_1) g_1(\mu_1) d\mu_1 \\ &+ b_1 \int_{\mu_1=M_1}^{x+M_1} F_{X_1}(x + M_1 - \mu_1) g_1(\mu_1) d\mu_1, \end{aligned} \quad (95)$$

where $g_1(x)$ is the derivative of $G_1(x)$, $F_{X_1}(x) = 1 - e^{-\lambda_1 x}$ is the CDF of X_1 . In addition, a_{11} is denoted by

$$a_{11} = p_1 + p_3 + (p_2 + p_4) e^{-\Omega_{SD}\Gamma_{th}} + \frac{p_4 (1 - e^{-\Omega_{SD}\Gamma_{th}}) e^{-\Omega_{R2D}\Gamma_{th}}}{M_2 b_2 \lambda_2}, \quad (96)$$

a_{12} is given by

$$a_{12} = \left[p_2 + p_4 \left(1 - \frac{1}{M_2 b_2 \lambda_2} \right) \right] (1 - e^{-\Omega_{SD}\Gamma_{th}}) + \frac{p_4 (1 - e^{-\Omega_{SD}\Gamma_{th}}) (1 - e^{-\Omega_{R2D}\Gamma_{th}})}{M_2 b_2 \lambda_2}, \quad (97)$$

a_{13} is written by

$$\begin{aligned} a_{13} &= (1 - e^{-\Omega_{SD}\Gamma_{th}}) (1 - e^{-\Omega_{R1D}\Gamma_{th}}) \\ &\times \left[p_2 - p_2 (1 - e^{-\Omega_{SR2}\Gamma_{th}}) e^{-\Omega_{R1R2}\Gamma_{th}} \right. \\ &\left. + p_4 \left(1 - \frac{e^{-\Omega_{R2D}\Gamma_{th}}}{M_2 b_2 \lambda_2} \right) \right], \end{aligned} \quad (98)$$

and b_1 is denoted by

$$\begin{aligned} b_1 &= (1 - e^{-\Omega_{SD}\Gamma_{th}}) \left[p_2 e^{-\Omega_{R1D}\Gamma_{th}} \right. \\ &+ p_2 (1 - e^{-\Omega_{R1D}\Gamma_{th}}) (1 - e^{-\Omega_{SR2}\Gamma_{th}}) e^{-\Omega_{R1R2}\Gamma_{th}} \\ &\left. + p_4 e^{-\Omega_{R1D}\Gamma_{th}} \left(1 - \frac{e^{-\Omega_{R2D}\Gamma_{th}}}{M_2 b_2 \lambda_2} \right) \right]. \end{aligned} \quad (99)$$

Furthermore, the $g_1(x)$ is defined as follows

$$g_1(x) = \begin{cases} g_{11}(x), & 0 \leq x < M_1 \\ g_{12}(x), & x \geq M_1. \end{cases} \quad (100)$$

When $x \geq M_1$, substituting Eq. (100) into Eq. (95), the derivatives about x on both sides of Eq. (95) can be obtained as follows

$$\begin{aligned} g_{12}(x) &= (a_{11} + a_{12}) \int_{\mu_1=0}^{M_1} f_{X_1}(x - \mu_1) g_{11}(\mu_1) d\mu_1 \\ &+ (a_{11} + a_{13}) \int_{\mu_1=M_1}^x f_{X_1}(x - \mu_1) g_{12}(\mu_1) d\mu_1 \\ &+ b_1 \int_{\mu_1=M_1}^{x+M_1} f_{X_1}(x + M_1 - \mu_1) g_{12}(\mu_1) d\mu_1. \end{aligned} \quad (101)$$

From Eq. (111) to Eq. (112), it is easy to know

$$a_{11} + a_{12} = a_{11} + a_{13} + b_1 = p_1 + p_2 + p_3 + p_4 = 1. \quad (102)$$

Like $g_{22}(x)$ in appendix B, let $g_{12}(x) = k_1 e^{Q_1 x}$. Moreover, substituting $g_{12}(x) = k_1 e^{Q_1 x}$ and $f_{X_1}(x) = \lambda_1 e^{-\lambda_1 x}$ and Eq. (102) into Eq. (101), we get

$$\begin{aligned} k_1 e^{Q_1 x} &= \int_{\mu_1=0}^{M_1} \lambda_1 e^{-\lambda_1(x-\mu_1)} g_{11}(\mu_1) d\mu_1 \\ &+ (1 - b_1) \int_{\mu_1=M_1}^x \lambda_1 e^{-\lambda_1(x-\mu_1)} k_1 e^{Q_1 \mu_1} d\mu_1 \\ &+ b_1 \int_{\mu_1=M_1}^{x+M_1} \lambda_1 e^{-\lambda_1(x+M_1-\mu_1)} k_1 e^{Q_1 \mu_1} d\mu_1. \end{aligned} \quad (103)$$

Let $a_{11} + a_{13} = a_1$ and simplify Eq. (103), we obtain

$$k_1 e^{Q_1 x} = \lambda_1 e^{-\lambda_1 x} \int_{\mu_1=0}^{M_1} e^{\lambda_1 \mu_1} g_{11}(\mu_1) d\mu_1 - \frac{k_1 \lambda_1 e^{(Q_1 M_1 - \lambda_1 x)} (a_1 e^{\lambda_1 M_1} + b_1)}{\lambda_1 + Q_1} + \frac{\lambda_1 (a_1 + b_1 e^{Q_1 M_1}) k_1 e^{Q_1 x}}{\lambda_1 + Q_1}. \quad (104)$$

For Eq. (104) to hold, the following conditions need to be satisfied

$$\begin{cases} \frac{\lambda_1 (a_1 + b_1 e^{Q_1 M_1})}{\lambda_1 + Q_1} = 1, \\ \frac{k_1 e^{Q_1 M_1} (a_1 e^{\lambda_1 M_1} + b_1)}{\lambda_1 + Q_1} = \int_{\mu_1=0}^{M_1} e^{\lambda_1 \mu_1} g_{11}(\mu_1) d\mu_1. \end{cases} \quad (105a)$$

Similarly, the desirable solution Q_1 of Eq. (105a) for the finite distribution of $g_{12}(x)$ may be obtained by simplifying Eq. (105a) as follows

$$b_1 \lambda_1 e^{Q_1 M_1} = \lambda_1 - a_1 \lambda_1 + Q_1 = b_1 \lambda_1 + Q_1. \quad (106)$$

Using Lambert W function, the solution Q_1 of Eq. (106) may be obtained as follows

$$Q_1 = \frac{-W(-b_1 \lambda_1 M_1 e^{-b_1 \lambda_1 M_1})}{M_1} - b_1 \lambda_1, \quad b_1 \lambda_1 M_1 > 1, \quad (107)$$

where, since $b_1 \lambda_1 M_1 > 1$, $W(-b_1 \lambda_1 M_1 e^{-b_1 \lambda_1 M_1}) > -b_1 \lambda_1 M_1$. Furthermore, $Q_1 < 0$, which ensures the finite distribution of $g_{12}(x)$.

When $0 \leq x < M_1$, substituting Eq. (100) into Eq. (95), the derivatives about x on both sides of Eq. (95) can be obtained as follows

$$g_{11}(x) = b_1 \int_{\mu_1=M_1}^{x+M_1} f_{X_1}(x + M_1 - \mu_1) g_{12}(\mu_1) d\mu_1 + \int_{\mu_1=0}^x f_{X_1}(x - \mu_1) g_{11}(\mu_1) d\mu_1. \quad (108)$$

Substituting $g_{12}(x) = k_1 e^{Q_1 x}$ and $f_{X_1}(x) = \lambda_1 e^{-\lambda_1 x}$ into Eq. (108), we get

$$g_{11}(x) = \lambda_1 \int_{\mu_1=0}^x e^{-\lambda_1(x-\mu_1)} g_{11}(\mu_1) d\mu_1 + \frac{b_1 k_1 \lambda_1 e^{Q_1 M_1}}{\lambda_1 + Q_1} (e^{Q_1 x} - e^{-\lambda_1 x}). \quad (109)$$

Similar to $g_{21}(x)$ in appendix B, the solution of $g_{11}(x)$ may be given as follows

$$g_{11}(x) = \frac{b_1 k_1 \lambda_1 e^{Q_1 M_1}}{\lambda_1 + Q_1} (e^{Q_1 x} - e^{-\lambda_1 x}) + \lambda_1 \int_{t=0}^x \frac{b_1 k_1 \lambda_1 e^{Q_1 M_1}}{\lambda_1 + Q_1} (e^{Q_1 t} - e^{-\lambda_1 t}) dt = \frac{b_1 k_1 \lambda_1 e^{Q_1 M_1} (e^{Q_1 x} - 1)}{Q_1}. \quad (110)$$

Because of the unit area condition on $g_1(x)$, we have

$$\int_{x=0}^{\infty} g_1(x) dx = \int_{x=0}^{M_1} g_{11}(x) dx + \int_{x=M_1}^{\infty} g_{12}(x) dx = 1. \quad (111)$$

Substituting $g_{11}(x) = \frac{b_1 k_1 \lambda_1 e^{Q_1 M_1} (e^{Q_1 x} - 1)}{Q_1}$ and $g_{12}(x) = k_1 e^{Q_1 x}$ into Eq. (111), we arrive at

$$k_1 = \frac{-Q_1}{M_1 (b_1 \lambda_1 + Q_1)}. \quad (112)$$

Furthermore, according to Eq. (112), we have

$$g_{11}(x) = \frac{1 - e^{Q_1 x}}{M_1}. \quad (113)$$

Similar to the validation of Eq. (75b), according to Eq. (106), Eq. (112) and Eq. (113), the Eq. (105b) may be validated as follows

$$\begin{aligned} \int_{\mu_1=0}^{M_1} e^{\lambda_1 \mu_1} g_{11}(\mu_1) d\mu_1 &= \frac{(1 - e^{Q_1 M_1}) (b_1 + a_1 e^{\lambda_1 M_1})}{(\lambda_1 + Q_1) M_1} \\ &= \frac{-Q_1 (b_1 + a_1 e^{\lambda_1 M_1})}{(\lambda_1 + Q_1) M_1 b_1 \lambda_1} \\ &= \frac{-Q_1 e^{Q_1 M_1} (b_1 + a_1 e^{\lambda_1 M_1})}{M_1 (b_1 \lambda_1 + Q_1) (\lambda_1 + Q_1)} \\ &= \frac{k_1 e^{Q_1 M_1} (b_1 + a_1 e^{\lambda_1 M_1})}{\lambda_1 + Q_1}. \end{aligned} \quad (114)$$

Now, the validation of Eq. (105b) in Eq. (114) indicates that the unique solution $g_{11}(x)$ in Eq. (113) for Eq. (108) and the unique solution $g_{12}(x) = k_1 e^{Q_1 x}$ for Eq. (101) are obtained.

REFERENCES

- [1] F. Unlu, L. Wawrla, and A. Diaz, "Energy harvesting technologies for IoT edge devices," Jul. 2018. [Online]. Available: <http://www.iea-4e.org/>.
- [2] D. Niyato, D. I. Kim, M. Maso and Z. Han, "Wireless powered communication networks: Research directions and technological approaches," *IEEE Wirel. Commun.*, vol. 24, no. 6, pp. 88-97, Dec. 2017.
- [3] D. Sui, F. Hu, W. Zhou, M. Shao and M. Chen, "Relay selection for radio frequency energy-harvesting wireless body area network with buffer," *IEEE Internet Things J.*, vol. 5, no. 2, pp. 1100-1107, Apr. 2018.
- [4] A. Alsharoa, H. Ghazzai, A. E. Kamal and A. Kadri, "Optimization of a power splitting protocol for two-way multiple energy harvesting relay system," *IEEE Trans. Green Commun. Netw.*, vol. 1, no. 4, pp. 444-457, Dec. 2017.
- [5] Y. Zou, J. Zhu and X. Jiang, "Joint power splitting and relay selection in energy-harvesting communications for IoT networks," *IEEE Internet Things J.*, vol. 7, no. 1, pp. 584-597, Jan. 2020.
- [6] R. Morsi, D. S. Michalopoulos and R. Schober, "On-off transmission policy for wireless powered communication with energy storage," in *Proc. 48th Asilomar Conf. Signals, Syst. Comput.*, Pacific Grove, CA, USA, Nov. 2014, pp. 1676-1682.
- [7] R. Morsi, D. S. Michalopoulos and R. Schober, "Performance analysis of wireless powered communication with finite/infinite energy storage," in *Proc. IEEE Int. Conf. Commun. (ICC)*, London, UK, Jun. 2015, pp. 2469-2475.
- [8] R. Morsi, D. S. Michalopoulos and R. Schober, "Performance analysis of near-optimal energy buffer aided wireless powered communication," *IEEE Trans. Wirel. Commun.*, vol. 17, no. 2, pp. 863-881, Feb. 2018.
- [9] Y. Wu, L. p. Qian, L. Huang and X. Shen, "Optimal relay selection and power control for energy-harvesting wireless relay networks," *IEEE Trans. Green Commun. Netw.*, vol. 2, no. 2, pp. 471-481, Jun. 2018.
- [10] S. Modem and S. Prakriya, "Optimization of two-way relaying networks with battery-assisted EH relays," *IEEE Trans. Commun.*, vol. 66, no. 10, pp. 4414-4430, Oct. 2018.
- [11] M. Moradian, F. Ashtiani and Y. J. Zhang, "Optimal relaying in energy harvesting wireless networks with wireless-powered relays," *IEEE Trans. Green Commun. Netw.*, vol. 3, no. 4, pp. 1072-1086, Dec. 2019.
- [12] C. -H. Lin and K. -H. Liu, "Relay selection for energy-harvesting relays with finite data buffer and energy storage," *IEEE Internet Things J.*, vol. 8, no. 14, pp. 11249-11259, Jul. 2021.

- [13] D. S. Gurjar, H. H. Nguyen and H. D. Tuan, "Wireless information and power transfer for IoT applications in overlay cognitive radio networks," *IEEE Internet Things J.*, vol. 6, no. 2, pp. 3257-3270, Apr. 2019.
- [14] Y. Ma, H. Chen, Z. Lin, Y. Li and B. Vucetic, "Distributed and optimal resource allocation for power beacon-assisted wireless-powered communications," *IEEE Trans. Commun.*, vol. 63, no. 10, pp. 3569-3583, Oct. 2015.
- [15] D. Bapatla and S. Prakriya, "Performance of incremental relaying with an energy-buffer aided relay," in *Proc. IEEE 89th Veh. Technol. Conf. (VTC2019-Spring)*, Kuala Lumpur, Malaysia, Apr. 2019, pp. 1-5.
- [16] D. Bapatla and S. Prakriya, "Performance of a cooperative network with an energy buffer-aided relay," *IEEE Trans. Green Commun. Netw.*, vol. 3, no. 3, pp. 774-788, Sep. 2019.
- [17] D. Bapatla and S. Prakriya, "Performance of energy-buffer aided incremental relaying in cooperative networks," *IEEE Trans. Wirel. Commun.*, vol. 18, no. 7, pp. 3583-3598, Jul. 2019.
- [18] D. Bapatla and S. Prakriya, "Performance of a cooperative network with energy harvesting source and relay," in *Proc. IEEE 90th Veh. Technol. Conf. (VTC2019-Fall)*, Honolulu, HI, USA, Sep. 2019, pp. 1-6.
- [19] D. Bapatla and S. Prakriya, "Performance of a cooperative communication network with green self-sustaining nodes," *IEEE Trans. Green Commun. Netw.*, vol. 5, no. 1, pp. 426-441, Mar. 2021.
- [20] D. Bapatla and S. Prakriya, "Performance of networks with an energy buffer-aided source and a data buffer-aided relay," in *Proc. IEEE 31st Annu. Int. Symp. Pers. Indoor Mobile Radio Commun.*, London, UK, Aug. 2020, pp. 1-5.
- [21] D. Bapatla and S. Prakriya, "Performance of two-hop links with an energy buffer-aided IoT source and a data buffer-aided relay," *IEEE Internet Things J.*, vol. 8, no. 6, pp. 5045-5061, Mar. 2021.
- [22] B. S. Awoyemi, A. S. Alfa and B. T. Maharaj, "Network restoration in wireless sensor networks for next-generation applications," *IEEE Sens. J.*, vol. 19, no. 18, pp. 8352-8363, Sep. 2019.
- [23] J. Zuo, C. Dong, H. V. Nguyen, S. X. Ng, L. Yang and L. Hanzo, "Cross-layer aided energy-efficient opportunistic routing in Ad Hoc networks," *IEEE Trans. Commun.*, vol. 62, no. 2, pp. 522-535, Feb. 2014.
- [24] J. Zuo, C. Dong, S. X. Ng, L. Yang and L. Hanzo, "Cross-layer aided energy-efficient routing design for Ad Hoc networks," *IEEE Commun. Surv. Tutor.*, vol. 17, no. 3, pp. 1214-1238, 3rd Quart., 2015.
- [25] X. Zhang, L. Tao, F. Yan and D. K. Sung, "Shortest-latency opportunistic routing in asynchronous wireless sensor networks with independent duty-cycling," *IEEE Trans. Mob. Comput.*, vol. 19, no. 3, pp. 711-723, Mar. 2020.
- [26] N. Li, J. Yan, Z. Zhang, J. -F. Martínez-Ortega and X. Yuan, "Geographical and topology control-based opportunistic routing for Ad Hoc networks," *IEEE Sens. J.*, vol. 21, no. 6, pp. 8691-8704, Mar. 2021.
- [27] N. Li, X. Yuan, J. -F. Martinez-Ortega and V. H. Diaz, "The network-based candidate forwarding set optimization for opportunistic routing," *IEEE Sens. J.*, vol. 21, no. 20, pp. 23626-23644, Oct. 2021.
- [28] R. W. L. Coutinho and A. Boukerche, "OMUS: Efficient opportunistic routing in multi-modal underwater sensor networks," *IEEE Trans. Wirel. Commun.*, vol. 20, no. 9, pp. 5642-5655, Sept. 2021.
- [29] Y. Zhang, Z. Zhang, L. Chen and X. Wang, "Reinforcement learning-based opportunistic routing protocol for underwater acoustic sensor networks," *IEEE Trans. Veh. Technol.*, vol. 70, no. 3, pp. 2756-2770, Mar. 2021.
- [30] S. Luo, R. Zhang and T. J. Lim, "Optimal save-then-transmit protocol for energy harvesting wireless transmitters," *IEEE Trans. Wirel. Commun.*, vol. 12, no. 3, pp. 1196-1207, Mar. 2013.
- [31] B. Zhang, C. Dong, M. El-Hajjar and L. Hanzo, "Outage analysis and optimization in single- and multiuser wireless energy harvesting networks," *IEEE Trans. Veh. Technol.*, vol. 65, no. 3, pp. 1464-1476, Mar. 2016.
- [32] S. Sudevalayam and P. Kulkarni, "Energy harvesting sensor nodes: Survey and implications," *IEEE Commun. Surv. Tutor.*, vol. 13, no. 3, pp. 443-461, 3rd Quart., 2011.
- [33] R. Loynes, "The stability of a queue with non-independent inter-arrival and service times," *Math. Proc. Cambridge Philos. Soc.*, vol. 58, no. 3, pp. 497-520, Jul. 1962.
- [34] A. Polyanin and A. Manzhirov, *Handbook of integral equations: Second edition, ser. handbooks of mathematical equations*. Taylor & Francis, 2008.